Game-theoretic solutions through intelligent optimization for efficient resource management in wireless visual sensor networks

Katerina Pandremmenou [a,*], Lisimachos P. Kondi [a,♣],
Konstantinos E. Parsopoulos [a], Elizabeth S. Bentley [b]

[a] *Department of Computer Science & Engineering, University of Ioannina, GR-45110 Ioannina, Greece*
[b] *Air Force Research Laboratory, Rome, NY, USA*

A R T I C L E   I N F O

A B S T R A C T

We propose a quality-driven cross-layer optimization scheme for wireless direct sequence code division multiple access (DS-CDMA) visual sensor networks (VSNs). The scheme takes into account the fact that different nodes image videos with varying amounts of motion and determines the source coding rate, channel coding rate, and power level for each node under constraints on the available bit rate and power. The objective is to maximize the quality of the video received by the centralized control unit (CCU) from each node. However, since increasing the power level of one node will lead to increased interference with the rest of the nodes, simultaneous maximization of the video qualities of all nodes is not possible. In fact, there are an infinite number of Pareto-optimal solutions. Thus, we propose the use of the Nash bargaining solution (NBS), which pinpoints one of the infinite Pareto-optimal solutions, based on the stipulation that the solution should satisfy four fairness axioms. The NBS results in a mixed-integer optimization problem, which is solved using the particle swarm optimization (PSO) algorithm. The presented experimental results demonstrate the advantages of the NBS compared with alternative optimization criteria.

© 2014 Elsevier B.V. All rights reserved.

1. Introduction

Wireless video communications suffer from a number of network resource constraints, including bandwidth, energy and computational complexity limitations. Data imaging, processing and transmission are recognized as power-consuming operations that can affect the performance of *visual sensor networks* (VSNs). Also, the available bit rate for video transmission can be limited in a wireless channel due to limited bandwidth and adverse channel conditions. VSNs consist of a number of spatially distributed nodes, each one equipped with a camera. The nodes are able to image and detect fields of different motion levels, depending on the specific application. The main challenge in VSNs is the coordinated behavior of each node constituting the network, such that it maximizes the overall system performance within the various resource constraints.

In general, game theory expands in two sharply different directions, namely non-cooperative game theory and cooperative game theory. The first branch is mainly concerned with the mutual interactions among intelligent individuals, striving to achieve their own goals. Several applications of non-cooperative game theory in wireless

* Corresponding author.
 E-mail addresses: apandrem@cs.uoi.gr (K. Pandremmenou),
lkon@cs.uoi.gr (L.P. Kondi), kostasp@cs.uoi.gr (K.E. Parsopoulos),
Elizabeth.Bentley@rl.af.mil (E.S. Bentley).
 ♣ EURASIP member.

networks are provided in [1–4]. In all these works, the Nash equilibrium appears as the solution achieved when the players compete with each other. A Nash equilibrium is reached when the strategy of each player is the best response to the strategies of the other players. However, such selfish behaviors often lead to suboptimal solutions, in the sense that user collaboration could promote an improved outcome, favorable for all players of the game.

In5 cooperative game theory models, the players coordinate their strategies by forming coalitions, in order to agree on a mutually acceptable division of the payoff. This aspect of game theory is also used in wireless networks for obtaining unbiased and efficient resource allocation schemes, avoiding disproportional allocations or resource depletion. Cooperative game theory concepts have been used to solve the opportunistic spectrum access problem [5]. Also, the issue of multi-radio resource allocation in generic heterogeneous wireless networks has been addressed based on the idea of network technologies cooperation [6]. Moreover, bargaining theory, which is highly associated with cooperative game theory, was applied to distribute resources at a relay node to multiple source nodes [7]. In [8], the problem of downlink resource allocation for a multi-user multiple-input multiple-output orthogonal frequency division multiple access system was considered through the bargaining perspective, while different fairness policies targeting at efficient resource management have been proposed [9–11].

The different nodes of a wireless VSN image videos with varying amounts of motion. When the employed network access method is the *direct sequence code division multiple access* (DS-CDMA), all nodes can transmit at the same time, sharing the same available bandwidth. However, a node transmission causes interference to the transmissions of the other nodes, deteriorating the quality of the video they transmit. If a node captures a video with low motion, then it may use fewer bits for source coding (video compression). This will leave more bits available for channel coding. Stronger channel coding will allow the transmission to tolerate a higher bit error rate. Thus, the transmission power of that node may be lower.

On the other hand, if a node captures a video with high motion, it will use more bits for source coding and fewer bits for channel coding, thus requiring a higher transmission power. Aiming at the achievement of high video quality, the transmission power should be adequately high to permit reliable data transmission and maintain the quality of the video reception. On the contrary, given that sensor nodes are battery-operated systems, it needs to be low enough to enhance the battery life of the nodes and keep interference to the other nodes' transmissions to low levels.

Additionally, DS-CDMA systems are interference limited and do not have a fixed limit on the number of users that can access the channel. Hence, low-motion nodes that transmit at low power will cause limited interference with the rest of the nodes, thus maintaining good overall system performance and allowing a larger number of nodes to use the channel. Thus, our consideration of the level of motion in the captured videos in the optimization makes DS-CDMA a clear choice as a wireless multiple access system.

In our previous work [12], we proposed a cross-layer optimization algorithm, under a centralized setting [13–15],

able to select the source coding rate, channel coding rate, and power level for each node, assuming constraints on the available bit rate and power. The objective was the maximization of the quality of the videos received by the *centralized control unit* (CCU) from each node. For this purpose, in [12] we used two optimization criteria; the *minimized average distortion* (MAD) criterion and the *minimized maximum distortion* (MMD) criterion.

As it is declared by their names, the MAD and MMD minimize the average and the maximum distortion of the nodes, respectively. Thus, they are rather focused on the overall or worst-case behavior of the network. Also, in [12], all parameters to be optimized (source coding rates, channel coding rates, power levels) assumed values from discrete sets. Therefore, a combinatorial optimization problem was formulated and solved. Furthermore, the MAD and MMD criteria were also used in [16], where the power levels assumed values from a continuous set, resulting in a mixed-integer optimization problem, which was solved using the *particle swarm optimization* (PSO) algorithm.

In [17], we applied axiomatic bargaining game theory [18], which belongs to the broader category of cooperative games. Axiomatic bargaining defines the properties (axioms) that shall be adhered to by the optimal solution, and they serve as criteria for rejecting other candidate solutions, until a unique optimal solution is finally selected. Specifically, in [17], we proposed the use of the *Nash bargaining solution* (NBS) in the game of resource allocation in a wireless VSN that uses DS-CDMA. In that work [17], the *disagreement point* (dp), which is the vector of minimum utilities that each node expects by joining the game without cooperating with the other nodes, was assumed to be the Nash equilibrium. Furthermore, finding the NBS involves solving an optimization problem where the Nash product is maximized. In the same paper [17], all parameters to be optimized (source coding rates, channel coding rates, power levels) were assumed to take values from discrete sets.

In the present paper, we apply cooperative game theory by using the Nash bargaining solution. The objective is to ameliorate the quality of the videos received by the CCU from each node, taking into account the fact that different nodes image videos with varying amounts of motion. Since the simultaneous maximization of the video qualities of all nodes is not possible, we employ the NBS in order to pinpoint one of the infinite Pareto-optimal solutions, based on the stipulation that the solution should satisfy four fairness axioms. Specifically, this solution promises fairness for all nodes, taking into account the amounts of motion in the videos they capture.

Compared to our previous work [17], the current paper deals with a mixed-integer optimization problem, since it involves both continuous (power levels) and discrete (source coding rates and channel coding rates) nodes' transmission parameters. Clearly, allowing power levels to take values from a continuous set offers flexibility to the CCU to perform better management of the nodes' transmission parameters, achieving in this way better end-to-end video quality for each node. Additionally, driven by the fact that, in a considered game, users' collaboration promotes improved outcomes favorable for all players participating in the game, in this work, we take careful treatment to the optimal setting

of the disagreement point. Particularly here, it is set by the system designer and it is does not correspond to the Nash equilibrium.

A preliminary version of this paper was presented in [19]. However, compared to [19], the current paper brings the following contributions. We introduce two versions of the NBS that differ in the definition of the bargaining powers. The first variant (NNBS) treats equally each individual node of the VSN, while the second variant (CNBS) provides equal treatment to each class of nodes. The proposed optimization schemes can be used for any wireless VSN with a centralized topology that uses DS-CDMA for data transmission. They keep low computational complexity, especially after the assumption of node clustering, based on the amounts of the detected motion in the videos recorded by the nodes. Given this assumption, fewer parameters need to be estimated and thus, less time is required for their computation. Additionally, the specific schemes not only provide Pareto-optimal solutions, but also guarantee fairness for all nodes of the VSN, as their fairness axioms state.

Traditional optimization algorithms on mixed-integer problems like the ones of this work may exhibit declining performance. For example, traditionally, infeasible primal-dual interior-point methods have had two main perceived deficiencies, i.e., lack of infeasibility detection capabilities, and poor performance after a warmstart [20]. On the other hand, specialized solutions may require significant implementation effort and expertise. Alternatively, such problems can be straightforwardly addressed by stochastic, population-based algorithms. Our previous experience with the particle swarm optimization algorithm [21] has verified its potential to tackle these optimization tasks [16,19], efficiently and effectively. Due to this, in this work we apply the PSO algorithm to the problem indicated by the NBS, under a cooperative game-theoretical perspective.

For the sake of paper's completeness, the performance of PSO is compared here with the performance of three deterministic optimization methods, which were used as benchmarks, such as *active-set* (AS) [22,23], *interior-point* (IP) [24,25] and *trust-region-reflective* (TRR) [26,27]. The conducted statistical tests showed that PSO greatly outperforms these classical deterministic algorithms, offering strong motivation for its use as the main optimizer in this work.

Additionally, in this paper, we experiment with various dp values in order to find this value that behaves equally fairly to each node and do not favor more some specific nodes. Also, the optimization problems of this work are of higher dimension compared to our previous works and our proposed methods are tested for more diverse parameter settings. The accuracy of the obtained results confirmed our belief that the NBS can be applied to any similar application in a wireless DS-CDMA VSN.

The rest of the paper is structured as follows: Section 2 provides a description of the network infrastructure considered in our study. Source and channel coding issues as well as the model used for the estimation of the video distortion are analyzed in Section 3. Section 4 is devoted to the proposed game-theoretic approaches, while Section 5 offers a brief presentation of PSO. Section 6 exposes the experimental part of our study, including configuration of

system parameters as well as presentation and interpretation of the obtained results. Finally, Section 7 summarizes the key concepts of the study and highlights the derived conclusions.

2. Network infrastructure

In this section, we present the cross-layer design as well as the wireless channel access method adopted in the considered network.

2.1. Cross-layer design

The cross-layer design used in the considered wireless VSN differs from the standard models like open systems interconnection or transmission control protocol/internet protocol. In these traditional architectures, a set of defined layers interact with each other, following the strict ordering of the assumed layer hierarchy. In contrast, the proposed design allows even non-adjacent layers to interact with each other and exchange information. The use of such a flexible scheme optimizes the end-to-end system performance, overcoming possible network latency problems.

The use of the cross-layer design is essential in this paper since the received video quality depends on decisions made at different network layers. The multi-node cross-layer technique assumes that the physical, data link, network and application layers cooperate with each other, optimizing network performance. At the physical layer, the transmission powers of all nodes are determined, while at the data link layer, the optimal channel coding rates are selected. At the application layer, the compression rates are chosen. The layer collaboration is coordinated by a centralized control unit, which undertakes to communicate with all nodes in order to request changes in transmission parameters, according to their unique, content-aware needs for resources. Fig. 1 gives an insight of a wireless VSN with two diverse video priorities.

2.2. Direct sequence code division multiple access

The current work assumes that the nodes can access the wireless VSN using the DS-CDMA channel access method. In DS-CDMA, all nodes transmit over the same bandwidth, while the transmission of each node is distinguished by the use of a different spreading code. An advantage of such systems is the lack of fixed limit on the number of nodes accessing the same bandwidth. However, a node transmission causes interference to the transmissions of the other nodes. Therefore, we are interested in achieving the ideal tradeoff between power consumption and video viewing quality. On one hand, spending less power will limit interference but, on the other hand, low power amounts cannot guarantee sufficient video quality. Hence, power control is considered indispensable for a successful DS-CDMA system.

The power S_k, henceforth called power level, of node k, refers to the power received by the CCU from node k. It is defined as $S_k = E_k R_k$ and is measured in Watts (W). The quantity E_k is the energy-per-bit and R_k is the total bit rate utilized for both source and channel coding. The required
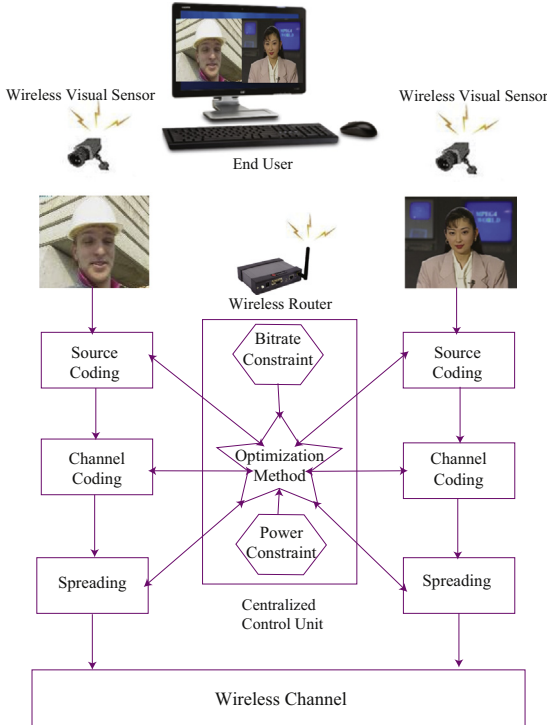
Fig. 1. A wireless VSN with two diverse video priorities.

transmission power $S_{k_{\text{trans}}}$ that will yield a power level S_k at the receiver is determined by a power control algorithm that is present in all practical DS-CDMA systems [28,29]. Power control can track the attenuation due to the distance between transmitter and receiver, as well as the effects of fading. The bit rate for node k is given by the fraction $R_k = R_{s,k}/R_{c,k}$, where $R_{s,k}$ represents the source coding rate and $R_{c,k}$ stands for the channel coding rate. The quantities $R_{s,k}$ and R_k are measured in bits per second (bps), and $R_{c,k}$, which is the ratio of the information bits over the total number of bits, is dimensionless, i.e., a single number without units of measure [30].

DS-CDMA systems are interference-limited [28]. Thus, it is common to assume that the thermal and background noise is negligible compared to the interference [31,32]. Furthermore, we assume that the interference can be approximated by additive white Gaussian noise [28,31,33]. We define the energy-per-bit to *multiple access interference* (MAI) ratio as

$$\frac{E_k}{I_0} = \frac{S_k/R_k}{\sum_{j=1,j\neq k}^{K} S_j/W_t}, \quad k = 1, 2, \ldots, K, \tag{1}$$

where $I_0/2$ is the two-sided power spectral density due to MAI, measured in Watts/Hertz (W/Hz). The quantity W_t denotes the total bandwidth, measured in Hertz (Hz). The subscript k refers to the current node, while j refers to the interfering nodes.

3. Video coding and the expected distortion

In this section, the source and channel coding characteristics are presented along with a discussion of the considered model for calculating the expected video distortion.

3.1. Source and channel coding

Source and channel coding are both necessary processes for video encoding. Source coding faces the challenge of video data representation with the smallest possible number of bits, ensuring tolerable levels of image quality degradation. In our study, the *H.264/advanced video coding* (H.264/AVC) standard was used to efficiently compress the video sequences imaged by the nodes. This standard can provide good video quality at substantially lower bit rates than earlier standards [34]. More specifically, the H.264/AVC Main profile was employed. This profile was designed so as to provide high coding efficiency. Therefore, it includes B-pictures, context-adaptive binary arithmetic coding, context-adaptive variable-length coding and interlaced coding tools. As the error rates after forward error correction are not expected to be high, the error resilience tools, i.e., flexible macroblock ordering, arbitrary slice order, and redundant slices, are not included in this profile [35].

Regarding channel coding, it aims to increase system resistance to channel errors by adding redundant bits to a video sequence. In this paper, channel coding is accomplished by the use of *rate compatible punctured convolutional* codes (RCPC codes) [36], which are families of codes with different rates that can be decoded by the same Viterbi decoder. However, other channel coding schemes can also be used.

We use Viterbi's upper bound of the bit error probability, P_b, for RCPC codes [31,36–38], which satisfies the relation

$$P_b \leq \frac{1}{P} \sum_{d=d_{\text{free}}}^{\infty} c_d P_d, \tag{2}$$

with

$$P_d = \frac{1}{2} \, \text{erfc}\left(\sqrt{\frac{dR_c E_k}{I_0}}\right), \tag{3}$$

and

$$\text{erfc}(x) = \frac{2}{\sqrt{\pi}} \int_x^{\infty} \exp(-t^2)\, dt. \tag{4}$$

In Rel. (2), the parameter P is the period of the code; d_{free} is the free distance of the code and c_d is the information error weight. In an additive white Gaussian noise channel that uses the binary phase shift keying modulation scheme, P_d is the probability that the wrong path at distance d is selected. In Eq. (3), the parameter R_c is the channel coding rate and E_k/I_0 is the energy-per-bit to MAI ratio, for node k. The complementary error function denoted as erfc(), is given by Eq. (4).

3.2. Modeling and estimation of the expected distortion

The video sequences received by the CCU are degraded by both the lossy compression and the errors introduced by the channel. Clearly, there is a direct relationship between the bit error rate (bit error probability), P_b, and the distortion of the video sequences. In this work, for the estimation

of the expected video distortion, $E[D_{s+c,k}]$, for node k, we used *universal rate-distortion characteristics* (URDC) [30]. These characteristics show the expected distortion, $E[D_{s+c,k}]$, as a function of the bit error probability, P_b, after channel decoding. However, since video encoded with the H.264 codec is designed to handle packet errors as opposed to bit errors, we need to calculate the resulting *packet loss rate* (PLR). We assume that the video bit stream is packetized using the *real-time transport protocol* (RTP). RTP provides a packet format for real-time data transmissions [39]. We calculate an RTP PLR from a certain *bit error rate* (BER), drop packets from the H.264 bitstream according to the RTP PLR, and pass the corrupted H.264 bitstream to the H.264 decoder to calculate the distortion of the video [12].

We assume that each RTP packet consists of a number of link layer packets. The link layer packet size is LL_{size}, measured in bits. Thus, the link layer PLR is $PLR_{LL} = 1 - (1 - BER)^{LL_{size}}$, where PLR_{LL} is the PLR for a link layer packet of size LL_{size}. Similarly, we calculate the RTP PLR with $PLR_{RTP} = 1 - (1 - PLR_{LL})^{RTP_{size}}$, where PLR_{RTP} is the PLR for an RTP packet of size RTP_{size}, measured in the number of link layer packets. We assume that we know when a packet has an error and we manually drop packets with any errors from the H.264 encoded video stream, in accordance with the PLR_{RTP} calculated from the BER.

Since channel errors are random, the video distortion $D_{s+c,k}$ of node k, which is due to both the lossy compression and channel errors, is a random variable. Thus, it does not suffice to calculate the video distortion for just one realization of the channel. Therefore, we will consider the expected value of the distortion, $E[D_{s+c,k}]$. Alternatively, instead of running repeated simulations in order to estimate the expected distortion at the receiver, it is also possible to estimate the expected distortion using the recursive optimal per-pixel estimate algorithm [40].

The URDC model used in this work to estimate the expected distortion is [12,19]

$$E[D_{s+c,k}] = \alpha \left[\log_{10} \left(\frac{1}{P_b} \right) \right]^{-\beta}, \qquad (5)$$

for node k. The parameters α and β are positive and they are highly dependent on the video content characteristics

clear that source and channel coding rates are inversely related quantities, i.e., higher source coding rates imply fewer bits available for channel coding, and vice versa.

Concerning the values that the source coding rates and channel coding rates can assume, it suffices to mention that the channel coding rates can only take discrete values from a set $\mathbf{R}_c$ [36]. Combining this assumption with the definition of R_k, this implies that source coding rates can also take discrete values from a set $\mathbf{R}_s$. On the contrary, the power levels assume continuous values from a predetermined range, namely $S_k \in \mathbf{P} = [s_{min}, s_{max}] \subset \mathbb{R}_+^*$, meaning that the power level values are bounded between s_{min} and s_{max}.

Let us assume that the pair $(R_{s,k}, R_{c,k})$ takes discrete values from a set:

$$\mathbf{R}_{s+c} = \{(R_s^1, R_c^1), (R_s^2, R_c^2), \dots, (R_s^M, R_c^M)\},$$

where the cardinality of $\mathbf{R}_{s+c}$ is equal to M. Hence, the sets $\mathbf{R}_s$, $\mathbf{R}_c$ and $\mathbf{R}_{s+c}$, have the same cardinality. Increasing the cardinality of one of these sets would considerably increase the corresponding optimization problem's search space, further complicating the problem. Additionally, cb_k denotes the index of the selected source–channel coding rate combination, for node k. For example, $cb_k = 1$ corresponds to the source–channel coding rate (R_s^1, R_c^1).

Since the parameters α and β in the URDC model, for node k, are functions of the source coding rate, they are immediately dependent on cb_k. Furthermore, the aforementioned parameters are also closely related to the motion detected in each video sequence. Higher motion levels detected in a video sequence or higher source coding rates correspond to higher values for the parameter α. The free distance of the code, d_{free}, and the information error weight, c_d, in P_b's equation depend on the channel coding rate and, thus, they are also dependent on cb_k. Viterbi's upper bound of Rel. (2) is considered to be tight [38], thus it can be used as an approximation of the bit error rate P_b [31]. To be noted that taking Rel. (2) with equality refers to a worst case analysis.

Substituting P_d into Rel. (2) (assuming it holds as equality), and then P_b into Eq. (5), $E[D_{s+c,k}]$ becomes

$$E[D_{s+c,k}](R_{s,k}, R_{c,k}, S) = \alpha(cb_k) \left[\log_{10} \frac{1}{\frac{1}{P} \sum_{d=d_{free}(cb_k)}^{\infty} \left(c_d(cb_k) \frac{1}{2} \ \mathrm{erfc} \left(\sqrt{dR_{c,k} \left(\frac{S_k/R_k}{\sum_{j=1, j \neq k}^{K} S_j/W_t} \right)} \right) \right)} \right]^{-\beta(cb_k)}, \qquad (6)$$

as well as the source coding rate. Their values are determined in a preprocessing phase by using mean squared error optimization for some $(E[D_{s+c,k}], P_b)$ pairs [12].

A significant constraint considered in our problem setup refers to the total bit rate used by each node for both source and channel coding. Specifically, each node shall transmit data using the same maximum bit rate. This constraint results from a fixed overall transmission chip rate, R_{chip}, measured in chips per second, and using the same spreading code length L, measured in chips, for all nodes, since $R_k = R_{chip}/L$. From the definition of R_k, it is

for node k. Evidently, the expected video distortion is a function of the source coding rate, $R_{s,k}$, and the channel coding rate, $R_{c,k}$, for node k, as well as of the power levels, $S = (S_1, S_2, \dots, S_K)^\top$, of all K nodes participating in the network.

4. Proposed game-theoretic approaches

In the following, we present the proposed game-theoretic approaches, after a brief introduction of the necessary background information. In order to reduce the

computational complexity of the solution, we assumed that the K nodes of the network are clustered into C motion classes, based on the amount of motion in the videos detected by the nodes.

4.1. Background information

The utility function, U_{cl}, constitutes a measure of relative satisfaction for each motion class cl. In our problem, it is defined equivalently to the *peak signal to noise ratio* (PSNR) [19]:

$$U_{cl} = 10 \log_{10} \frac{255^2}{E[D_{s+c,cl}]}, \quad cl = 1, 2, \dots, C, \tag{7}$$

and thus, it is measured in decibel (dB). The quantity $E[D_{s+c,cl}]$ represents the expected video distortion for motion class cl, given by Eq. (6). Clearly, higher values of the utility function correspond to higher received video qualities.

The vector $U = (U_1, U_2, \dots, U_C)^\top$ contains the utilities for all C motion classes. The feasible set, $\mathbf{U}$, encompasses all possible vectors U that result from all possible combinations of the source and channel coding rates as well as the power levels of all motion classes, when pure strategies are allowed. (A pure strategy defines a deterministic action of a player.) Also, it shall satisfy the following conditions [5]:

(1) $\mathbf{U} \subset \mathbb{R}^C$ is comprehensive, closed and bounded-above.
(2) Free disposal is allowed.

The first condition stipulates that a set $\mathbf{U} \subset \mathbb{R}^C$ shall be comprehensive. This means that if X is in $\mathbf{U}$ and $Y \leq X$, then Y is in $\mathbf{U}$ as well [41]. Additionally, the same set shall also include all its boundary points (i.e., be closed) and be bounded from above. A set $\mathbf{U}$ is bounded-above, if there exists X such that $Y \leq X$ for all $Y \in \mathbf{U}$.

Regarding the second condition, free disposal means that each player is permitted to dispose of utility, if required. The physical meaning in the case of video is that a class of nodes is allowed to purposely add noise to its video to degrade the video quality. Obviously, this is an irrational decision and will never be chosen. However, in our formulation we should not restrict the possible choices of the players regarding the handling of their resources, unless they lead to cases that are impossible to be implemented. Specifically, if $Y \leq X$, and X is a feasible point for all classes of nodes, it follows that Y can be achieved by the players also by mutually agreeing to dispose of utility, unilaterally or multilaterally. In this paper, we assume that free disposal is allowed for the feasible set and therefore, this statement clearly implies that the feasible set $\mathbf{U}$ is also comprehensive [5,41].

Each player expects by participating in a game that it will receive at least as high a utility as it would get without joining the game (without collaborating). This fact constitutes an incentive for the players to negotiate. The disagreement point is the vector of minimum utilities that each player expects by joining the game without cooperating with the other players, and it is what each player will get even in cases of negotiation failure. It is defined as $dp = (dp_1, dp_2, \dots, dp_C)^\top$, for all C players (classes of nodes), and it also belongs to the feasible set.

The outcome of a game is said to be Pareto-optimal if there is no other outcome that concurrently favors all players. In this work, we refer to Pareto-optimality in the strong sense, which implies that there is no other outcome where at least one player strictly increases its utility and no player decreases its utility. The Pareto-optimal points, which are members of the feasible set and give each node a utility that is greater than or equal to the disagreement point, form the bargaining set.

4.2. Nash bargaining solution

In our problem, the Nash bargaining solution offers a distribution rule in order to achieve a mutually agreeable, fair and efficient allocation of the node classes' transmission parameters. Specifically, the NBS, denoted as $F(\mathbf{U}, dp)$ for the feasible set $\mathbf{U}$ and the disagreement point dp, shall adhere to the following axioms [41]:

(1) *Individual rationality*: $F(\mathbf{U}, dp) \geq dp$.
(2) *Pareto-optimality*: $X > F(\mathbf{U}, dp) \Rightarrow X \notin \mathbf{U}$.
(3) *Invariance to affine transformations*: Given any strictly increasing affine transformation $\tau()$, it holds that $F(\tau(\mathbf{U}), \tau(dp)) = \tau(F(\mathbf{U}, dp))$.
(4) *Independence of irrelevant alternatives*: If $dp \in \mathbf{Y} \subseteq \mathbf{U}$, then $F(\mathbf{U}, dp) \in \mathbf{Y} \Rightarrow F(\mathbf{Y}, dp) = F(\mathbf{U}, dp)$.

The first two axioms imply that the NBS belongs to the bargaining set and the third axiom stipulates that the NBS is unaffected by affine transformation scalings of the utility function. The last axiom states that, if the bargaining solution, $F(\mathbf{U}, dp)$, for the feasible set $\mathbf{U}$ also belongs to a subset $\mathbf{Y}$ of the feasible set, then $F(\mathbf{Y}, dp)$ shall be the same as $F(\mathbf{U}, dp)$, since none of the extra elements of $\mathbf{U}$ were chosen as a solution when they were available. Thus, their unavailability in $\mathbf{Y}$ should be irrelevant.

Provided that the aforementioned conditions are satisfied, the NBS maximizes the Nash product [5,19,41]:

$$F(\mathbf{U}, dp) = \arg \max_{U \geq dp} \prod_{cl=1}^{C} (U_{cl}(R_{s,cl}, R_{c,cl}, S) - dp_{cl})^{a_{cl}}, \tag{8}$$

subject to the following constraints:

1. $R_k = R_{\text{target}}$ (fixed bit rate).
2. $S_{cl} \in \mathbf{P} = [s_{\min}, s_{\max}] \subset \mathbb{R}_+^*$ (bounded power).
3. $\sum_{cl=1}^{C} a_{cl} = 1, a_{cl} \geq 0, \; cl = 1, 2, \dots, C$.

The parameter a_{cl} assigned to each factor of the Nash product is called bargaining power and declares the advantage of each player in the considered game. Higher bargaining powers imply more advantaged players, and vice versa.

Since the determination of the bargaining powers is crucial for the performance and efficiency of the NBS, in this paper we propose two versions of the NBS, the NNBS and the CNBS. For the NNBS, we assume that each node

has the same advantage in the resource allocation game. Practically, given the constraint that the sum of all bargaining powers is equal to 1, and considering an equally fair game for all nodes, it follows that each class of nodes cl is assigned a bargaining power equal to $a_{cl} = 1/K_{cl}$, with K_{cl} representing the cardinality of class cl. For the CNBS, we assumed that each class of nodes is put in a similar position by the rules of the considered game. Therefore, assuming C motion classes, and considering the constraint for the total sum of the bargaining powers, it is implied that $a_{cl} = 1/C$, for the cl class of nodes.

Apart from the bargaining powers, another component that directly affects the Nash product is the disagreement point, as derived from Eq. (8). For this reason, we shall pay attention to the appropriate determination of this vector. In [17], we assumed that the disagreement point corresponds to the vector of utilities that the motion classes get if they behave selfishly, without collaborating with each other. Following this reasoning, a class of nodes that desire to achieve the best possible received video quality regardless of the intentions of the other classes will have to transmit using the maximum power. However, if all motion classes adopt this strategy, they will all select to transmit at maximum power, thereby reaching a Nash equilibrium. This occurs since each motion class adopts the strategy that is the best response to the strategies followed by the other classes.

However, such a selection for the disagreement point heavily favors the classes of nodes that capture videos with low motion, which get high utility and have no incentive to collaborate [17]. For this reason, in the present study we assume that the disagreement point is imposed by the system designer and expresses the minimum acceptable video quality for each class of nodes, for the particular application.

5. Particle swarm optimization

Particle swarm optimization was initially introduced by Eberhart and Kennedy [42,43], as a stochastic algorithm for numerical optimization tasks. PSO uses a population, called swarm, of search points, called particles, to probe the search space, simultaneously. Each particle assumes an adaptable velocity to move in the search space. The velocity has the meaning of an adaptable position-shift, rather than the corresponding physical vector quantity.

Moreover, each particle retains a memory of the best position it has ever visited, i.e., the position with the lowest function value. This is the particle's experience to be shared with its neighboring particles. For this purpose, each particle is assigned a neighborhood, namely a set of other particles, which defines its information-sharing neighboring particles. Actually, the neighborhood is denoted as a set of indices of its neighboring particles that will share its experience, while it can also be depicted as a graph of nodes, representing the particles, and edges, representing their communication channels. The pattern that defines the communication paths is often called neighborhood's topology.

Putting it formally, assume the n-dimensional continuous optimization problem:

$$\min_{x \in \mathbf{X} \subset \mathbb{R}^n} f(x).$$

A swarm of N particles is a set of search points, $\mathbf{S} = \{x_1, x_2, ..., x_N\}$, where the i-th particle is defined as

$$x_i = (x_{i1}, x_{i2}, ..., x_{in})^\top \in \mathbf{X}, \quad i \in \mathbf{I} = \{1, 2, ..., N\}.$$

The velocity (position-shift) of x_i is denoted as

$$v_i = (v_{i1}, v_{i2}, ..., v_{in})^\top, \quad i \in \mathbf{I},$$

and its best position as

$$p_i = (p_{i1}, p_{i2}, ..., p_{in})^\top \in \mathbf{X}, \quad i \in \mathbf{I}.$$

In the present paper, we adopted the ring neighborhood topology. If r denotes the neighborhood's radius, the neighborhood of the i-th particle is defined as

$$\mathcal{N}_i = \{i-r, ..., i-1, i, i+1, ..., i+r\},$$

with indices recycling at the ends of their limits.

Let g_i denote the index of the best particle in $\mathcal{N}_i$, i.e., $g_i = \arg\min_{j \in \mathcal{N}_i} f(p_j)$, and t denotes the algorithm's iteration counter. Then, the particle positions and velocities are updated at each iteration according to the equations [44]:

$$v_{ij}^{(t+1)} = \chi[v_{ij}^{(t)} + c_1 R_1 (p_{ij}^{(t)} - x_{ij}^{(t)}) + c_2 R_2 (p_{g_i j}^{(t)} - x_{ij}^{(t)})], \tag{9}$$

$$x_{ij}^{(t+1)} = x_{ij}^{(t)} + v_{ij}^{(t+1)}, \tag{10}$$

$$i = 1, 2, ..., N \text{ and } j = 1, 2, ..., n,$$

where χ is the constriction coefficient; c_1 and c_2 are positive constants called cognitive and social parameter, respectively; and R_1, R_2, are random numbers drawn from a uniform distribution in the range $[0, 1]$. The PSO model defined in Eqs. (9) and (10) was proposed by Clerc and Kennedy in [44], and is considered as a state-of-the-art PSO variant. For this reason, we adopted this model in the paper at hand.

The best position of each particle is updated as follows:

$$p_{ij}^{(t+1)} = \begin{cases} x_{ij}^{(t+1)} & \text{if } f(x_{ij}^{(t+1)}) < f(p_{ij}^{(t)}), \\ p_{ij}^{(t)} & \text{otherwise}. \end{cases} \tag{11}$$

Clerc and Kennedy [44] offered a thorough stability and convergence analysis of the presented PSO model. Based on this analysis, the parameter set $\chi = 0.729$, and $c_1 = c_2 = 2.05$, has been considered as the default configuration. Alternative configurations were proposed by Trelea in [45]. The swarm and velocities are usually initialized randomly and uniformly within the search space.

6. System setup and experimental results

This section exposes the configuration of the system parameters, experimental results and discussion. The results from the NBS approaches were assessed in comparison with the results from the MAD and MMD criteria, studied in [16].
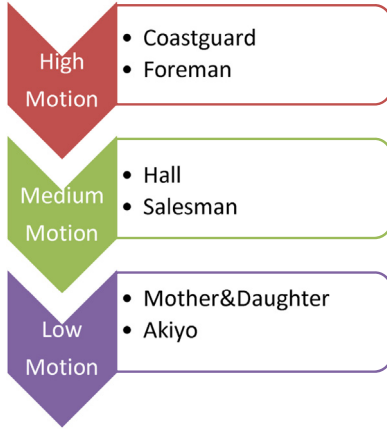
Fig. 2. The used video sequences and the amount of motion described by each of them.

6.1. Configuration of system parameters

The VSN considered in this paper consisted of $K=102$ nodes, which capture videos of various amounts of motion. In order to simulate the various amounts of motion included in the videos, we used a number of video sequences, which were downloaded from [46]. The video sequences used as well as the amount of motion in each one is depicted in Fig. 2.

All video sequences were at *quarter common intermediate format* (QCIF) resolution and were encoded at 15 frames per second. From the "Salesman" video sequence we kept only the first 300 frames in order to have the same length for all video sequences.

Additionally, we assumed that the K nodes of the VSN are clustered into $C=6$ motion classes, with each sequence being a representative of a motion class. For the node distributions into the six motion classes we considered the following cases:

- *Case* 1: $K_a = K_{md} = K_s = K_h = K_f = K_c = 17$.
- *Case* 2: $K_a = K_{md} = 25, K_s = K_h = K_f = K_c = 13$.
- *Case* 3: $K_a = K_{md} = K_f = K_c = 13, K_s = K_h = 25$.
- *Case* 4: $K_a = K_{md} = K_s = K_h = 13, K_f = K_c = 25$.

K_a denotes the cardinality of the class that is represented by the "Akiyo" video sequence, while K_{md}, K_s, K_h, K_f and K_c denote the cardinality of the class that is represented by the "Mother&Daughter", "Salesman", "Hall", "Foreman" and "Coastguard" video sequences, respectively. In all four node distributions described above, the total number of nodes is equal to $K=102$ nodes. In Case 1, all classes include exactly the same number of nodes; in Case 2 more nodes describe low amounts of motion; in Case 3 more nodes describe medium amounts of motion and in Case 4 more nodes describe high amounts of motion. For the assessment of the perceived visual quality of the video sequences, the PSNR video quality metric was used, which is equal to the utility function of Eq. (7), and is measured in dB.

The RCPC codes used for channel coding had a mother code of rate 1/4 [36]. Also, two different cases were considered for the bit rate R_k: (i) 96 kbps and (ii) 144 kbps. Taking into account these bit rate constraints, it follows that the source–channel coding rate combinations can take the following discrete values:

(i) $R_k = 96$ kbps

$$\mathbf{R}_{s+c} = \{(32, 1/3), (38.4, 4/10), (48, 1/2), (64, 2/3), (76.8, 4/5)\}$$
$$cb_{cl} = 1 \longrightarrow (32, 1/3)$$
$$cb_{cl} = 2 \longrightarrow (38.4, 4/10)$$
$$cb_{cl} = 3 \longrightarrow (48, 1/2)$$
$$cb_{cl} = 4 \longrightarrow (64, 2/3)$$
$$cb_{cl} = 5 \longrightarrow (76.8, 4/5)$$

(ii) $R_k = 144$ kbps

$$\mathbf{R}_{s+c} = \{(48, 1/3), (57.6, 4/10), (72, 1/2), (96, 2/3), (115.2, 4/5)\}$$
$$cb_{cl} = 1 \longrightarrow (48, 1/3)$$
$$cb_{cl} = 2 \longrightarrow (57.6, 4/10)$$
$$cb_{cl} = 3 \longrightarrow (72, 1/2)$$
$$cb_{cl} = 4 \longrightarrow (96, 2/3)$$
$$cb_{cl} = 5 \longrightarrow (115.2, 4/5).$$

The index $cl \in \{a, md, s, h, f, c\}$ denotes the class of nodes that is represented by the "Akiyo", "Mother&Daughter", "Salesman", "Hall", "Foreman" and "Coastguard" video sequence, respectively. Concerning the power levels, they can take continuous values from the set $\mathbf{P} = [5.0, 15.0]$, measured in Watts (W). For the bandwidth, W_t, we examined the following values per bit rate constraint, R_k:

(1) $R_k = 96$ kbps   (2) $R_k = 144$ kbps
(a) $W_t = 20$ MHz   (a) $W_t = 30$ MHz
(b) $W_t = 15$ MHz   (b) $W_t = 22.5$ MHz.

Since $R_k = 144$ kbps is 1.5 times the $R_k = 96$ kbps, the same reasoning was followed for the bandwidth values. Specifically, $W_t = 30$ MHz is 1.5 times the $W_t = 20$ MHz and $W_t = 22.5$ MHz is 1.5 times the $W_t = 15$ MHz. This corresponds to keeping the spreading code length the same for both cases.

In order to maximize the Nash product, PSO is used to minimize its negative. Specifically:

$$f(x) = -((U_a(cb_a, S_a) - dp_a)^{a_a} \cdot (U_{md}(cb_{md}, S_{md}) - dp_{md})^{a_{md}}$$
$$\cdot (U_s(cb_s, S_s) - dp_s)^{a_s} \cdot (U_h(cb_h, S_h) - dp_h)^{a_h}$$
$$\cdot (U_f(cb_f, S_f) - dp_f)^{a_f} \cdot (U_c(cb_c, S_c) - dp_c)^{a_c}), \quad (12)$$

where the particle $x = (S_a, S_{md}, S_s, S_h, S_f, S_c, cb_a, cb_{md}, cb_s, cb_h, cb_f, cb_c)^{\top}$ consists of the power levels, as well as the combinations of source and channel coding rates, for all motion classes. The discrete components of the particle, i.e., the source and channel coding rate combinations, cb_a, cb_{md}, cb_s, cb_h, cb_f, cb_c, were let to assume continuous values within the range $\mathbf{R} = [0.6, 5.4]$. However, they were rounded to the nearest integer whenever the particle was evaluated.

Regarding PSO, identical parameter settings were used for both NNBS and CNBS criteria. Specifically, the default parameter set defined in Section 5 was selected and a swarm of $N=100$ particles following the ring topology with radius $r=1$ was used. Moreover, since PSO is a stochastic algorithm, its performance was evaluated over

Table 1
PSNR values for different dp, using PSO, for $R_k=96$ kbps and $W_t=20$ MHz.

	Sequences	NNBS				CNBS			
		$dp=28$	$dp=27$	$dp=26$	$dp=25$	$dp=28$	$dp=27$	$dp=26$	$dp=25$
Case 1	"Akiyo"	36.5112	36.6797	36.8173	36.9319	36.5112	36.6797	36.8173	36.9319
	"Mother&Daughter"	34.5452	34.6279	34.6957	34.7521	34.5452	34.6279	34.6957	34.7521
	"Salesman"	33.0986	33.0871	33.0777	33.0697	33.0986	33.0871	33.0777	33.0697
	"Hall"	33.8855	33.9285	33.9637	33.9929	33.8855	33.9285	33.9637	33.9929
	"Foreman"	33.5774	33.6097	33.6378	33.6621	33.5774	33.6097	33.6378	33.6621
	"Coastguard"	**31.7825**	31.6143	31.4685	31.3413	**31.7825**	31.6143	31.4685	31.3413
Case 2	"Akiyo"	36.9809	36.8912	37.1221	37.2022	36.9424	36.9382	36.9356	36.9334
	"Mother&Daughter"	34.9393	34.8361	34.9994	35.0243	33.6715	33.6401	33.6110	33.5875
	"Salesman"	33.3904	33.2421	33.3045	33.2733	33.6637	33.6380	33.6148	33.5940
	"Hall"	34.2718	35.2623	35.4899	35.5408	35.8310	35.9345	36.0190	36.0895
	"Foreman"	35.0184	34.8631	35.1263	35.1739	**35.3444**	35.3347	35.3289	35.3239
	"Coastguard"	**32.8463**	32.6105	31.7981	31.6474	**32.7816**	32.7745	32.7702	32.7665
Case 3	"Akiyo"	36.9558	36.8917	37.0031	37.1001	37.4139	37.5529	37.6663	37.7609
	"Mother&Daughter"	34.8905	34.8361	34.8806	34.9213	35.4221	35.4903	35.5448	35.5896
	"Salesman"	33.3543	33.2422	33.2158	33.1963	32.8240	32.8028	32.7937	32.7862
	"Hall"	34.2239	34.1341	35.3394	35.4096	33.1350	33.0680	33.0095	32.9582
	"Foreman"	34.0659	34.8633	33.9198	33.9284	**35.7753**	35.7898	35.7631	35.7409
	"Coastguard"	**32.8041**	32.6106	31.6680	31.5307	**33.1541**	33.1083	33.0887	33.0725
Case 4	"Akiyo"	35.8036	36.1377	36.3882	36.5839	37.0979	37.5082	37.8145	38.0531
	"Mother&Daughter"	33.8701	34.0992	34.2704	34.4030	35.1134	35.4458	35.6941	35.8869
	"Salesman"	32.5969	32.6923	32.7593	32.8080	33.5191	33.6951	33.8216	33.9162
	"Hall"	33.2280	33.4080	33.5419	33.6446	35.5853	36.0320	36.3737	36.6444
	"Foreman"	32.6798	32.8640	33.0096	33.1267	**30.7193**	30.5880	30.4715	30.3670
	"Coastguard"	**30.1005**	29.8555	29.6511	29.4783	**29.8901**	29.6107	29.3772	29.1796

Table 2
PSNR values for different dp, using PSO, for $R_k=96$ kbps and $W_t=15$ MHz.

	Sequences	NNBS				CNBS			
		$dp=26$	$dp=25$	$dp=24$	$dp=23$	$dp=26$	$dp=25$	$dp=24$	$dp=23$
Case 1	"Akiyo"	35.6945	35.9260	36.1113	36.2636	35.6945	35.9260	36.1113	36.2636
	"Mother&Daughter"	33.5979	33.7564	33.8830	33.9863	33.5979	33.7564	33.8830	33.9863
	"Salesman"	32.2508	32.3180	32.3695	32.4100	32.2508	32.3180	32.3695	32.4100
	"Hall"	32.8823	33.0063	33.1049	33.1850	32.8823	33.0063	33.1049	33.1850
	"Foreman"	**30.2644**	30.1824	30.1099	30.0453	**30.2644**	30.1824	30.1099	30.0453
	"Coastguard"	**29.2214**	29.0370	28.8818	28.7496	**29.2214**	29.0370	28.8818	28.7496
Case 2	"Akiyo"	36.1434	36.3211	36.4657	36.5859	35.3258	35.3934	35.2294	35.4980
	"Mother&Daughter"	34.0389	34.1504	34.2403	34.3142	32.5165	32.5537	33.0002	32.6025
	"Salesman"	32.5823	32.6143	32.6382	32.6564	32.7412	32.7807	33.1431	32.8332
	"Hall"	33.3179	33.3982	33.4622	33.5142	33.5278	33.6192	34.1380	33.7512
	"Foreman"	**30.6672**	30.5615	30.4680	30.3847	32.5214	32.6343	31.1627	32.8104
	"Coastguard"	**29.5215**	29.3229	29.1539	29.0087	**29.6692**	29.4868	29.6795	29.1970
Case 3	"Akiyo"	36.0155	36.2113	36.3704	36.5026	36.3045	36.4973	36.6539	36.7839
	"Mother&Daughter"	33.9130	34.0407	34.1441	34.2294	34.1980	34.3268	34.4307	34.5161
	"Salesman"	32.4877	32.5319	32.5659	32.5927	31.5356	31.5615	31.5818	31.5980
	"Hall"	33.1933	33.2889	33.3659	33.4290	31.7751	31.7760	31.7738	31.7697
	"Foreman"	**30.5507**	30.4550	30.3709	30.2964	32.8400	32.8961	32.9403	32.9756
	"Coastguard"	**29.4348**	29.2427	29.0802	28.9414	**29.6321**	29.4531	29.3008	29.1699
Case 4	"Akiyo"	34.9081	35.2441	35.5041	35.7124	35.8943	36.2671	36.5527	36.7796
	"Mother&Daughter"	32.8337	33.0818	33.2741	33.4280	33.7938	34.0965	34.3282	34.5117
	"Salesman"	31.6736	31.8085	31.9101	31.9892	32.3982	32.5737	32.7042	32.8046
	"Hall"	32.1320	32.3380	32.4979	32.6256	33.0756	33.3444	33.5502	33.7129
	"Foreman"	**29.5999**	29.5560	29.5162	29.4799	**29.0024**	28.8656	28.7452	28.6382
	"Coastguard"	**28.7254**	28.5630	28.4288	28.3160	**28.2780**	28.0378	27.8366	27.6658

30 independent experiments. At each experiment, the algorithm was executed for $Iter=700$ iterations (which correspond to 70,000 function evaluations for the 100 particles) and the best solution was recorded. Hence, taking into account that the number of particles (N) and the number of iterations ($Iter$) both depend on the number of motion classes (C), the complexity of PSO is $O(C \cdot N \cdot Iter)$.

6.2. Presentation and discussion of results

We first explore the effect of the value of the disagreement point vector in the results of the NBS-based criteria. Tables 1–4 show the achieved PSNR values for the NNBS and CNBS criteria, using the PSO as the optimization solver. We test different selections of the dp vector, for the same bit rate and bandwidth combination. The tested values for the vector of the dp are also different for each bit rate and bandwidth combination, since they must be feasible values using the available bit rate and bandwidth, at each time. Additionally, all the elements of a dp vector were equal. Although this is not obligatory, we made this assumption in an effort to be equally fair to all motion classes.

In practice, video that includes high amounts of motion is particularly important in surveillance applications, since this is where the action occurs. From the presented experimental results, we confirmed that increasing the values of the dp vector results in favoring the nodes that image high motion levels more than the rest of the nodes, a fact that is expounded by the achieved PSNR values for each motion class. This is what the values in bold denote in Tables 1–4. In addition, the amelioration of the

video quality becomes more perceivable in videos with poor quality rather than in videos with good visual quality. Therefore, we assigned to dp the highest values among the tested ones for each combination of bit rate and bandwidth. Thus, all our experiments with the NNBS and CNBS have been conducted using:

(i) $dp=28$ dB for the cases:
    (a) $R_k=96$ kbps and $W_t=20$ MHz.
    (b) $R_k=144$ kbps and $W_t=30$ MHz.
(ii) $dp=26$ dB for the cases:
    (a) $R_k=96$ kbps and $W_t=15$ MHz.
    (b) $R_k=144$ kbps and $W_t=22.5$ MHz.

In Tables 5–8 we report the results for the four different node distributions and all considered criteria, solved by PSO, for all bit rate and bandwidth combinations. The reported quantities at each line of the tables are the power level, S, the combination of source and channel coding rate, (R_s, R_c), and the achieved utility, PSNR, per class. The values in bold refer to the total power levels and achieved PSNR values for all node distributions and criteria.

Studying the performance of NNBS and CNBS, we observe that when all motion classes have the same cardinality (Case 1), both NBS approaches offer exactly the same solution, i.e, the same PSNR values to all motion classes. In Case 2, the NNBS offers higher PSNR values compared to the CNBS, to the nodes that describe low amounts of motion. In Case 3, the same criterion (NNBS) assigns higher PSNR values compared to the CNBS, to the nodes that describe medium amounts of motion and in

Table 3
PSNR values for different dp, using PSO, for $R_k=144$ kbps and $W_t=30$ MHz.

	Sequences	NNBS				CNBS			
		dp = 28	dp = 27	dp = 26	dp = 25	dp = 28	dp = 27	dp = 26	dp = 25
Case 1	"Akiyo"	36.4608	36.7424	36.9780	37.1782	36.4608	36.7424	36.9780	37.1782
	"Mother&Daughter"	34.5607	34.7048	34.8257	34.9284	34.5607	34.7048	34.8257	34.9284
	"Salesman"	33.6832	33.7449	33.7959	33.8382	33.6832	33.7449	33.7959	33.8382
	"Hall"	34.0215	34.1143	34.1915	34.2564	34.0215	34.1143	34.1915	34.2564
	"Foreman"	33.5108	33.5653	33.6114	33.6504	33.5108	33.5653	33.6114	33.6504
	"Coastguard"	**30.9488**	30.6709	30.4247	30.2056	**30.9488**	30.6709	30.4247	30.2056
Case 2	"Akiyo"	36.9372	37.4978	37.6764	37.8302	35.3652	35.4299	35.4863	35.5358
	"Mother&Daughter"	34.9906	35.4015	35.4793	35.5459	33.5877	33.5149	33.4510	33.3944
	"Salesman"	34.0740	34.3847	34.4003	34.4124	34.9117	34.9451	34.9743	34.9999
	"Hall"	34.4212	34.7646	34.8034	34.8357	35.2744	35.3324	35.3829	35.4272
	"Foreman"	33.9734	34.3446	34.3610	34.3739	34.9981	35.0481	35.0932	35.1340
	"Coastguard"	**32.7052**	31.1199	30.8668	30.6401	**33.5649**	33.4763	33.3962	33.3237
Case 3	"Akiyo"	36.9433	37.1866	37.3925	37.5692	37.6623	37.9145	38.1293	38.3148
	"Mother&Daughter"	34.9962	35.1135	35.2129	35.2982	35.6522	35.7891	35.9063	36.0077
	"Salesman"	34.0791	34.1199	34.1538	34.1819	32.6142	32.4898	32.3800	32.2823
	"Hall"	34.4263	34.4957	34.5540	34.6033	32.9227	32.8314	32.7509	32.6794
	"Foreman"	33.9795	34.0190	34.0526	34.0812	34.7077	34.7907	34.8639	34.9287
	"Coastguard"	**31.2108**	30.9324	30.6851	30.4646	**33.3202**	33.2569	33.1990	33.1457
Case 4	"Akiyo"	35.4595	35.9111	36.2769	36.5806	36.6970	37.2631	37.7171	38.0907
	"Mother&Daughter"	33.6705	33.9479	34.1759	34.3666	34.7734	35.1841	35.5176	35.7938
	"Salesman"	32.8784	33.0533	33.1971	33.3171	33.8763	34.1849	34.4358	34.6434
	"Hall"	33.1952	33.4086	33.5836	33.7294	34.2192	34.5617	34.8392	35.0684
	"Foreman"	**31.6048**	31.5892	31.5741	31.5590	**30.8078**	30.6425	30.4941	30.3591
	"Coastguard"	**30.4360**	30.2016	29.9977	29.8190	**29.8923**	29.5397	29.2286	28.9526

Table 4
PSNR values for different dp, using PSO, for $R_k = 144$ kbps and $W_t = 22.5$ MHz.

	Sequences	NNBS				CNBS			
		dp = 26	dp = 25	dp = 24	dp = 23	dp = 26	dp = 25	dp = 24	dp = 23
Case 1	"Akiyo"	34.1645	34.4186	34.5889	34.6786	34.1645	34.4186	34.5889	34.6786
	"Mother&Daughter"	32.0453	32.1855	32.3602	32.5980	32.0453	32.1855	32.3602	32.5980
	"Salesman"	31.1217	31.1968	31.2682	31.3454	31.1217	31.1968	31.2682	31.3454
	"Hall"	31.5210	31.6229	31.8874	31.9786	31.5210	31.6229	31.8874	31.9786
	"Foreman"	**29.2876**	29.2015	29.0012	28.9201	**29.2876**	29.2015	29.0012	28.9201
	"Coastguard"	**28.0057**	27.7981	27.5629	27.3057	**28.0057**	27.7981	27.5629	27.3057
Case 2	"Akiyo"	34.8552	35.0496	35.2546	35.5378	33.1191	33.2324	33.3648	33.5678
	"Mother&Daughter"	32.6833	32.7767	32.9886	33.2501	31.0925	31.0872	31.2674	31.3897
	"Salesman"	31.7107	31.7459	31.8761	32.0452	32.6571	32.7461	32.8964	33.1562
	"Hall"	32.1199	32.1790	32.3564	32.5648	33.0788	33.1889	33.3617	33.4879
	"Foreman"	**29.8588**	29.7500	29.6420	29.5273	**30.8089**	30.7803	30.6348	30.2468
	"Coastguard"	**28.4254**	28.2047	28.1036	28.0010	**29.1200**	28.9639	28.7464	28.5560
Case 3	"Akiyo"	34.5609	34.7806	34.8978	35.1762	35.7362	36.0013	36.2564	36.5963
	"Mother&Daughter"	32.4107	32.5241	32.7896	32.9968	33.5056	33.6763	33.7888	34.2165
	"Salesman"	31.4588	31.5112	31.7862	31.9689	30.0895	30.0402	30.2658	30.5986
	"Hall"	31.8640	31.9414	32.3619	32.6891	30.4669	30.4470	30.6790	30.8970
	"Foreman"	**29.6126**	29.5140	29.3456	29.2165	**30.6207**	30.6106	30.0631	29.7532
	"Coastguard"	**28.2447**	28.0299	27.8962	27.6031	**28.9827**	28.8393	28.6866	28.4650
Case 4	"Akiyo"	33.0309	33.3978	33.5698	33.8938	34.4020	34.8576	35.1395	35.4443
	"Mother&Daughter"	31.0128	31.2392	31.0012	30.8964	32.2639	32.5963	32.3363	32.1161
	"Salesman"	30.1727	30.3207	30.6896	30.8896	31.3233	31.5783	31.8622	32.1116
	"Hall"	30.5520	30.7328	30.9863	31.3489	31.7262	32.0093	32.4658	32.6874
	"Foreman"	**28.4022**	28.3533	28.0130	27.7985	**27.4835**	27.3023	27.1542	26.9868
	"Coastguard"	**27.3516**	27.1656	26.8543	26.6366	**26.6678**	26.3748	26.2010	26.0012

Case 4, higher PSNR values are assigned to the nodes that describe high amounts of motion, using also the NNBS compared to the CNBS. In all other cases, the CNBS "beats" the NNBS, by assigning higher PSNR values compared to the latter.

Continuing, the performance of the NNBS and CNBS criteria was compared with the performance achieved by the MAD and MMD criteria proposed in our previous work [16]. The MAD criterion minimizes the average distortion of the videos received by all nodes. For the Cases 2 and 3, a wise selection between NNBS and CNBS can always give higher PSNR results compared to the MAD, to all motion classes. For Cases 1 and 4 the same can also be done, but with some exceptions.

The MMD criterion minimizes the maximum (worst) distortion among all the videos captured by the nodes and this solution is achieved when all nodes have the same distortion. In the considered DS-CDMA wireless VSN, reducing the distortion of a node by increasing its transmission power increases the interference with the other nodes and thus, their distortion is increased. Hence, if we want to minimize the worst distortion among the nodes, we have to increase the transmission power of the "worst" node. Typically, this criterion offers the same utilities to all nodes. From the obtained results we observe that the MMD in all examined cases assigns exactly the same PSNR values to both classes of nodes that describe high amounts of motion. Also, in the large majority of the cases, the same PSNR values are also assigned to the sequence/sequences that describe medium amounts of motion. Last but not least, there are also some cases where all motion classes enjoy exactly the same PSNR values.

However, these results reveal that there are some cases where some nodes receive a lower distortion than that of the other nodes. At the same time, in these cases, these nodes need the lowest possible transmission power. Specifically, they need 5.0000 W, which is the low bound of the considered power level range. As a result, these nodes achieve lower distortions than the rest of the nodes, despite the fact that they use the least possible power. Evidently, if we had allowed a smaller low bound for the power level range, the specific nodes would use even less power and thus, all nodes would receive exactly the same distortion (thus, the same PSNR).

Comparing the performance of the MMD criterion with the performance of the NNBS and CNBS criteria, the latter can be wisely used so as to assign higher PSNR values to the low and medium video sequences, with some exceptions for the case of $R_k = 96$ kbps and $W_t = 20$ MHz.

Additionally, the higher the amounts of motion included in a sequence, the higher the power level that is required and also, the lower the PSNR value that is achieved. At this point, we should point out that the PSO algorithm is able to detect a number of optimal solutions for the power levels of all motion classes, all of which can attain the optimum value for the Nash product. Indeed, from Eq. (1), it follows that the multiplication of all power levels with the same constant leaves the ratio E_k/I_0 unaffected. This is because we assumed that thermal and background noise is negligible compared with the interference. In our results, we have normalized the power levels so that the lowest allocated power is equal to 5.0000 W.

However, the source–channel coding rate combinations were unique in all examined cases. The nodes that

Table 5
Experimental results using PSO for $R_k = 96$ kbps and $W_t = 20$ MHz.

	Sequences	NNBS			CNBS			MAD			MMD		
		S	(R_s, R_c)	PSNR	S	(R_s, R_c)	PSNR	S	(R_s, R_c)	PSNR	S	(R_s, R_c)	PSNR
Case 1	"Akiyo"	5.0000	(32,1/3)	36.5112	5.0000	(32,1/3)	36.5112	5.0000	(32,1/3)	36.2808	5.0000	(32,1/3)	37.0690
	"Mother&Daughter"	6.1970	(32,1/3)	34.5452	6.1970	(32,1/3)	34.5452	6.3500	(32,1/3)	34.4621	5.0000	(32,1/3)	33.7349
	"Salesman"	5.8840	(32,1/3)	33.0986	5.8840	(32,1/3)	33.0986	6.2000	(32,1/3)	33.1756	5.2662	(32,1/3)	32.9946
	"Hall"	6.8140	(32,1/3)	33.8855	6.8140	(32,1/3)	33.8855	7.0500	(32,1/3)	33.8988	5.4199	(32,1/3)	32.9946
	"Foreman"	14.0260	(48,1/2)	33.5774	14.0260	(48,1/2)	33.5774	14.6000	(48,1/2)	33.6466	12.2326	(48,1/2)	32.9946
	"Coastguard"	14.4270	(48,1/2)	31.7825	14.4270	(48,1/2)	31.7825	15.0000	(48,1/2)	31.8157	15.0000	(64,2/3)	32.9946
	Total	**52.3480**		**203.4004**	**52.3480**		**203.4004**	**54.2118**		**203.2796**	**47.9187**		**202.7823**
Case 2	"Akiyo"	5.0000	(32,1/3)	36.9809	5.0000	(32,1/3)	36.9424	5.0000	(32,1/3)	36.9572	5.0000	(38.4,4/10)	35.0808
	"Mother&Daughter"	6.1387	(32,1/3)	34.9393	5.0555	(32,1/3)	33.6715	6.1150	(32,1/3)	34.8931	5.0000	(32,1/3)	34.2562
	"Salesman"	5.8296	(32,1/3)	33.3904	6.2451	(32,1/3)	33.6637	6.0468	(32,1/3)	33.5344	5.8396	(32,1/3)	33.8069
	"Hall"	6.7451	(32,1/3)	34.2718	8.3800	(38.4,4/10)	35.8310	6.8460	(32,1/3)	34.3374	5.6838	(32,1/3)	33.8069
	"Foreman"	14.5715	(64,2/3)	35.0184	15.0000	(64,2/3)	35.3444	14.5421	(64,2/3)	34.9341	12.0802	(48,1/2)	33.8069
	"Coastguard"	15.0000	(64,2/3)	32.8463	15.0000	(64,2/3)	32.7816	15.0000	(64,2/3)	32.8065	15.0000	(64,2/3)	33.8069
	Total	**53.2849**		**207.4471**	**54.6806**		**208.2346**	**53.5499**		**207.4627**	**48.6036**		**204.5646**
Case 3	"Akiyo"	5.0000	(32,1/3)	36.9558	5.2132	(32,1/3)	37.4139	5.0000	(32,1/3)	36.9399	5.0000	(32,1/3)	37.4428
	"Mother&Daughter"	6.1139	(32,1/3)	34.8905	6.4668	(32,1/3)	35.4221	6.0062	(32,1/3)	34.7674	5.0000	(32,1/3)	34.1410
	"Salesman"	5.8058	(32,1/3)	33.3543	5.0000	(32,1/3)	32.8240	5.9207	(32,1/3)	33.4298	5.7001	(32,1/3)	33.6265
	"Hall"	6.7184	(32,1/3)	34.2239	5.4524	(32,1/3)	33.1350	6.7194	(32,1/3)	34.2095	5.6214	(32,1/3)	33.6265
	"Foreman"	13.6258	(48,1/2)	34.0659	14.9177	(64,2/3)	35.7753	13.6744	(48,1/2)	34.0777	12.1153	(48,1/2)	33.6265
	"Coastguard"	15.0000	(64,2/3)	32.8041	15.0000	(64,2/3)	33.1541	15.0000	(64,2/3)	32.7774	15.0000	(64,2/3)	33.6265
	Total	**52.2636**		**206.2945**	**52.0501**		**207.7244**	**52.3207**		**206.2017**	**48.4368**		**206.0898**
Case 4	"Akiyo"	5.0000	(32,1/3)	35.8036	5.0000	(32,1/3)	37.0979	5.0000	(32,1/3)	35.6996	5.0000	(32,1/3)	36.0568
	"Mother&Daughter"	6.1890	(32,1/3)	33.8701	6.2010	(32,1/3)	35.1134	6.3910	(32,1/3)	33.9843	5.0000	(32,1/3)	32.6348
	"Salesman"	5.8750	(32,1/3)	32.5969	5.8895	(32,1/3)	33.5191	6.1889	(32,1/3)	32.7776	5.0000	(32,1/3)	31.9587
	"Hall"	6.8130	(32,1/3)	33.2280	7.9245	(38.4,4/10)	35.5853	7.1161	(32,1/3)	33.4128	5.1498	(32,1/3)	31.5385
	"Foreman"	14.4575	(48,1/2)	32.6798	9.4885	(32,1/3)	30.7193	15.0000	(48,1/2)	32.9506	12.6278	(32,1/3)	31.5385
	"Coastguard"	12.6450	(32,1/3)	30.1005	9.9345	(32,1/3)	29.8901	12.2593	(32,1/3)	29.8803	15.0000	(48,1/2)	31.5385
	Total	**50.9795**		**198.2789**	**44.4380**		**201.9251**	**51.9553**		**198.7052**	**47.7776**		**195.2658**

Table 6
Experimental results using PSO for $R_k=96$ kbps and $W_t=15$ MHz.

	Sequences	NNBS			CNBS			MAD			MMD		
		S	(R_s, R_c)	PSNR	S	(R_s, R_c)	PSNR	S	(R_s, R_c)	PSNR	S	(R_s, R_c)	PSNR
Case 1	"Akiyo"	5.0000	(32,1/3)	35.6945	5.0000	(32,1/3)	35.6945	5.0000	(32,1/3)	35.0168	5.0000	(32,1/3)	35.2312
	"Mother&Daughter"	6.0230	(32,1/3)	33.5979	6.0230	(32,1/3)	33.5979	6.4010	(32,1/3)	33.3981	5.0000	(32,1/3)	31.7377
	"Salesman"	5.5620	(32,1/3)	32.2508	5.5620	(32,1/3)	32.2508	6.1295	(32,1/3)	32.2877	5.0000	(32,1/3)	31.3134
	"Hall"	6.5455	(32,1/3)	32.8823	6.5455	(32,1/3)	32.8823	7.0970	(32,1/3)	32.8212	5.1860	(32,1/3)	30.6941
	"Foreman"	10.8655	(32,1/3)	30.2644	10.8655	(32,1/3)	30.2644	12.2990	(32,1/3)	30.4978	12.3134	(32,1/3)	30.6941
	"Coastguard"	10.6320	(32,1/3)	29.2214	10.6320	(32,1/3)	29.2214	11.9025	(32,1/3)	29.3379	15.0000	(48,1/2)	30.6941
	Total	**44.6280**		**193.9113**	**44.6280**		**193.9113**	**48.8290**		**193.3595**	**47.4994**		**190.3646**
Case 2	"Akiyo"	5.0000	(32,1/3)	36.1434	5.0000	(32,1/3)	35.3258	5.0000	(32,1/3)	35.2539	5.0000	(32,1/3)	35.8514
	"Mother&Daughter"	6.0360	(32,1/3)	34.0389	5.4467	(32,1/3)	32.5165	6.3586	(32,1/3)	33.5627	5.0000	(32,1/3)	32.4116
	"Salesman"	5.5710	(32,1/3)	32.5823	6.4488	(32,1/3)	32.7412	6.1069	(32,1/3)	32.4249	5.0000	(32,1/3)	31.7982
	"Hall"	6.5600	(32,1/3)	33.3179	7.5948	(32,1/3)	33.5278	7.0575	(32,1/3)	32.9887	5.2294	(32,1/3)	31.4334
	"Foreman"	10.8100	(32,1/3)	30.6672	15.0000	(48,1/2)	32.5214	15.0000	(48,1/2)	32.4018	12.6330	(32,1/3)	31.4334
	"Coastguard"	10.5830	(32,1/3)	29.5215	12.2136	(32,1/3)	29.6692	11.9233	(32,1/3)	29.5011	15.0000	(48,1/2)	31.4334
	Total	**44.5600**		**196.2712**	**51.7039**		**196.3019**	**51.4463**		**196.1331**	**47.8624**		**194.3614**
Case 3	"Akiyo"	5.0000	(32,1/3)	36.0155	5.5936	(32,1/3)	36.3045	5.0000	(32,1/3)	35.2806	5.0000	(32,1/3)	35.8273
	"Mother&Daughter"	6.0325	(32,1/3)	33.9130	6.7573	(32,1/3)	34.1980	6.4400	(32,1/3)	33.6732	5.0000	(32,1/3)	32.3854
	"Salesman"	5.5685	(32,1/3)	32.4877	5.0000	(32,1/3)	31.5356	6.1980	(32,1/3)	32.5171	5.0000	(32,1/3)	31.7793
	"Hall"	6.5560	(32,1/3)	33.1933	5.7320	(32,1/3)	31.7751	7.1535	(32,1/3)	33.1013	5.2272	(32,1/3)	31.4039
	"Foreman"	10.8230	(32,1/3)	30.5507	15.0000	(48,1/2)	32.8400	12.4530	(32,1/3)	30.8146	12.6201	(32,1/3)	31.4039
	"Coastguard"	10.5970	(32,1/3)	29.4348	11.8194	(32,1/3)	29.6321	12.1445	(32,1/3)	29.6109	15.0000	(48,1/2)	31.4039
	Total	**44.5770**		**195.5950**	**49.9023**		**196.2853**	**49.3890**		**194.9977**	**47.8473**		**194.2037**
Case 4	"Akiyo"	5.0000	(32,1/3)	34.9081	5.0000	(32,1/3)	35.8943	5.0000	(32,1/3)	34.3861	5.0000	(32,1/3)	33.7426
	"Mother&Daughter"	5.9965	(32,1/3)	32.8337	6.0290	(32,1/3)	33.7938	6.3065	(32,1/3)	32.7405	5.0000	(32,1/3)	30.1199
	"Salesman"	5.5440	(32,1/3)	31.6736	5.5665	(32,1/3)	32.3982	5.9745	(32,1/3)	31.7394	5.0000	(32,1/3)	30.1496
	"Hall"	6.5155	(32,1/3)	32.1320	6.5520	(32,1/3)	33.0756	6.9585	(32,1/3)	32.1522	5.5550	(32,1/3)	29.7558
	"Foreman"	10.9590	(32,1/3)	29.5999	8.8385	(32,1/3)	29.0024	11.9135	(32,1/3)	29.7447	12.8151	(32,1/3)	29.7558
	"Coastguard"	10.7140	(32,1/3)	28.7254	8.6335	(32,1/3)	28.2780	11.3330	(32,1/3)	28.6895	15.0000	(32,1/3)	29.7558
	Total	**44.7290**		**189.8727**	**40.6195**		**192.4423**	**47.4860**		**189.4522**	**48.3701**		**183.2795**

describe high motion usually use more bits to compress their data and leave fewer bits that can be used to protect the sequence from transmission errors. In the following, Tables 5–8 confirm our conviction that decreasing the bandwidth while keeping the bit rate constant, the value of Eq. (1) decreases, incurring a PSNR decrease to all motion classes.

For the total consumed power, there is no specific scheme that requires the highest amounts of power levels in all cases of a specific bit rate and bandwidth combination, except for the case of $R_k=144$ kbps and $W_t=22.5$ MHz, where the MMD criterion clearly needs far more power compared to the other schemes. Furthermore, it seems that Case 2 is the most demanding in resources (in terms of power) compared to the other three cases, when $R_k=96$ kbps and $W_t=20$ MHz, and $R_k=144$ kbps and $W_t=30$ MHz. The same holds also in half cases of $R_k=96$ kbps and $W_t=15$ MHz, and $R_k=144$ kbps and $W_t=22.5$ MHz. Last but not least, the highest total PSNR values are achieved in Case 2 of all examined bit rate and bandwidth combinations, with only an isolated exception.

All of the optimization criteria examined in this paper, i.e., the Nash bargaining solution (particularly here the two approaches NNBS and CNBS), the MAD and the MMD provide Pareto-optimal solutions. Specifically for the NBS, let us assume that the provided solution (the solutions from the NNBS and CNBS), i.e., the solution that maximizes the Nash product is not Pareto-optimal. This means that there is another solution where at least one node strictly increases its utility and no node decreases its utility. However, such a solution would lead to an even greater Nash product, thus contradicting the fact that the NBS maximizes the Nash product. Therefore, the solution provided by the NBS criterion is Pareto-optimal.

Similar reasoning applies also to the MAD criterion. If we assume that the solution given by the MAD is not Pareto-optimal, this means that there is another solution where at least one node receives lower distortion and no node increases its distortion. However, such a solution would lead to an even smaller average distortion, thus contradicting the fact that the MAD criterion minimizes the average distortion. Therefore, the solution provided by the MAD criterion is Pareto-optimal.

As mentioned earlier, the MMD solution occurs when an "equilibrium" is reached, i.e., when all nodes have the same distortion (except in some cases when a node, i.e., motion class, uses a power level at the lower end of the considered power level range), and, increasing a node's transmission power will increase the distortions of the other nodes, thus leading to a higher maximum distortion.

If the solution given by the MMD is not Pareto-optimal, this would mean that there exists another solution where

Table 7
Experimental results using PSO for $R_k = 144$ kbps and $W_t = 30$ MHz.

	Sequences	NNBS			CNBS			MAD			MMD		
		S	(R_s, R_c)	PSNR	S	(R_s, R_c)	PSNR	S	(R_s, R_c)	PSNR	S	(R_s, R_c)	PSNR
Case 1	"Akiyo"	5.0000	(48,1/3)	36.4608	5.0000	(48,1/3)	36.4608	5.0000	(48,1/3)	35.9137	5.0000	(48,1/3)	34.5798
	"Mother&Daughter"	6.0859	(48,1/3)	34.5607	6.0889	(48,1/3)	34.5607	6.3540	(48,1/3)	34.5109	6.3054	(48,1/3)	33.2093
	"Salesman"	6.5475	(48,1/3)	33.6832	6.5475	(48,1/3)	33.6832	6.9400	(48,1/3)	33.7930	7.3095	(48,1/3)	33.2093
	"Hall"	6.2033	(48,1/3)	34.0215	6.2033	(48,1/3)	34.0215	6.5390	(48,1/3)	34.0764	6.7042	(32,1/3)	33.2093
	"Foreman"	10.9137	(72,1/2)	33.5108	10.9137	(72,1/2)	33.5108	11.5525	(72,1/2)	33.6666	12.5330	(48,1/3)	33.2093
	"Coastguard"	10.4261	(48,1/3)	30.9488	10.4261	(48,1/3)	30.9488	10.9800	(48,1/3)	30.9864	15.0000	(48,1/3)	33.2093
	Total	**45.1795**		**203.1858**	**45.1795**		**203.1858**	**47.3655**		**202.9470**	**52.8521**		**200.6263**
Case 2	"Akiyo"	5.0000	(48,1/3)	36.9372	5.0000	(48,1/3)	35.3652	5.0000	(48,1/3)	36.3332	5.0000	(48,1/3)	35.5691
	"Mother&Daughter"	6.0765	(48,1/3)	34.9906	6.1183	(48,1/3)	33.5877	6.3770	(48,1/3)	34.9365	6.4225	(48,1/3)	34.3115
	"Salesman"	6.5275	(48,1/3)	34.0740	8.1458	(48,1/3)	34.9117	6.9825	(48,1/3)	34.2124	7.5287	(48,1/3)	34.3115
	"Hall"	6.1895	(48,1/3)	34.4212	7.7352	(48,1/3)	35.2744	6.5760	(48,1/3)	34.4928	6.8920	(48,1/3)	34.3115
	"Foreman"	10.7665	(72,1/2)	33.9734	13.1513	(72,1/2)	34.9981	11.4865	(72,1/2)	34.1553	12.3809	(72,1/2)	34.3115
	"Coastguard"	11.8530	(72,1/2)	32.7052	14.4449	(72,1/2)	33.5649	12.8185	(72,1/2)	33.0510	15.0000	(72,1/2)	34.3115
	Total	**46.4130**		**207.1016**	**54.5955**		**207.7020**	**49.2405**		**207.1812**	**53.2241**		**207.1266**
Case 3	"Akiyo"	5.0000	(48,1/3)	36.9433	5.0000	(48,1/3)	37.6623	5.0000	(48,1/3)	35.9637	5.0000	(48,1/3)	35.1208
	"Mother&Daughter"	6.0765	(48,1/3)	34.9962	6.0590	(48,1/3)	35.6522	6.3570	(48,1/3)	34.5617	6.3659	(48,1/3)	33.8065
	"Salesman"	6.5275	(48,1/3)	34.0791	5.2935	(48,1/3)	32.6142	6.9450	(48,1/3)	33.8430	7.4243	(48,1/3)	33.8065
	"Hall"	6.1890	(48,1/3)	34.4263	5.0040	(48,1/3)	32.9227	6.5435	(48,1/3)	34.1261	6.8021	(48,1/3)	33.8065
	"Foreman"	10.7650	(72,1/2)	33.9795	10.5535	(72,1/2)	34.7077	11.5450	(72,1/2)	33.7248	12.4494	(72,1/2)	33.8065
	"Coastguard"	10.3110	(48,1/3)	31.2108	11.5990	(72,1/2)	33.3202	12.8355	(72,1/2)	32.6268	15.0000	(72,1/2)	33.8065
	Total	**44.8690**		**205.6352**	**43.5090**		**206.8793**	**49.2260**		**204.8461**	**53.0417**		**204.1533**
Case 4	"Akiyo"	5.0000	(48,1/3)	35.4595	5.0000	(48,1/3)	36.6970	5.0000	(48,1/3)	35.1774	5.0000	(48,1/3)	32.9847
	"Mother&Daughter"	6.1155	(48,1/3)	33.6705	6.0830	(48,1/3)	34.7734	6.3125	(48,1/3)	33.7643	6.2398	(48,1/3)	31.6621
	"Salesman"	6.5910	(48,1/3)	32.8784	6.5375	(48,1/3)	33.8763	6.8640	(48,1/3)	33.0576	7.1215	(48,1/3)	31.6621
	"Hall"	6.2340	(48,1/3)	33.1952	6.1965	(48,1/3)	34.2192	6.4740	(48,1/3)	33.3461	6.5542	(48,1/3)	31.6621
	"Foreman"	10.3350	(48,1/3)	31.6048	8.7005	(48,1/3)	30.8078	10.7305	(48,1/3)	31.7761	12.5792	(48,1/3)	31.6621
	"Coastguard"	10.6795	(48,1/3)	30.4360	9.0040	(48,1/3)	29.8923	10.7025	(48,1/3)	30.2586	15.0000	(48,1/3)	31.6621
	Total	**44.9550**		**197.24444**	**41.5215**		**200.2660**	**46.0835**		**197.3801**	**52.4947**		**191.2952**

Table 8
Experimental results using PSO for $R_k = 144$ kbps and $W_t = 22.5$ MHz.

	Sequences	NNBS			CNBS			MAD			MMD		
		S	(R_s, R_c)	PSNR	S	(R_s, R_c)	PSNR	S	(R_s, R_c)	PSNR	S	(R_s, R_c)	PSNR
Case 1	"Akiyo"	5.0000	(48,1/3)	34.1645	5.0000	(48,1/3)	34.1645	5.0000	(48,1/3)	33.1807	5.0000	(48,1/3)	30.1623
	"Mother&Daughter"	5.8885	(48,1/3)	32.0453	5.8885	(48,1/3)	32.0453	6.1850	(48,1/3)	31.7519	6.6545	(48,1/3)	30.1623
	"Salesman"	6.1985	(48,1/3)	31.1217	6.1985	(48,1/3)	31.1217	6.6445	(48,1/3)	31.0805	7.4745	(48,1/3)	30.1623
	"Hall"	5.9185	(48,1/3)	31.5210	5.9185	(48,1/3)	31.5210	6.2885	(48,1/3)	31.3786	6.9120	(48,1/3)	30.1623
	"Foreman"	9.4195	(48,1/3)	29.2876	9.4195	(48,1/3)	29.2876	10.4010	(48,1/3)	29.6193	13.2165	(48,1/3)	30.1623
	"Coastguard"	8.8895	(48,1/3)	28.0057	8.8895	(48,1/3)	28.0057	9.9280	(48,1/3)	28.3462	14.8490	(48,1/3)	30.1623
	Total	**41.3145**		**186.1458**	**41.3145**		**186.1458**	**44.4470**		**185.3572**	**54.1065**		**180.9738**
Case 2	"Akiyo"	5.0000	(48,1/3)	34.8552	5.0000	(48,1/3)	33.1191	5.0000	(48,1/3)	33.8512	5.0000	(48,1/3)	31.7686
	"Mother&Daughter"	5.8840	(48,1/3)	32.6833	5.8950	(48,1/3)	31.0925	6.2265	(48,1/3)	32.4322	6.4705	(48,1/3)	31.0979
	"Salesman"	6.1905	(48,1/3)	31.7107	7.7055	(48,1/3)	32.6571	6.7150	(48,1/3)	31.7506	7.3337	(48,1/3)	31.0979
	"Hall"	5.9135	(48,1/3)	32.1199	7.3670	(48,1/3)	33.0788	6.3480	(48,1/3)	32.0442	6.7650	(48,1/3)	31.0979
	"Foreman"	9.3350	(48,1/3)	29.8588	11.4845	(48,1/3)	30.8089	10.5020	(48,1/3)	30.3640	12.8977	(48,1/3)	31.0979
	"Coastguard"	8.8210	(48,1/3)	28.4254	10.8730	(48,1/3)	29.1200	10.1715	(48,1/3)	29.0056	15.0000	(48,1/3)	31.0979
	Total	**41.1440**		**189.6533**	**48.2950**		**189.8764**	**44.9630**		**189.4478**	**53.4669**		**187.2581**
Case 3	"Akiyo"	5.0000	(48,1/3)	34.5609	5.2395	(48,1/3)	35.7362	5.0000	(48,1/3)	33.5194	5.0000	(48,1/3)	31.0367
	"Mother&Daughter"	5.8860	(48,1/3)	32.4107	6.1590	(48,1/3)	33.5056	6.2060	(48,1/3)	32.0955	6.5748	(48,1/3)	30.7007
	"Salesman"	6.1940	(48,1/3)	31.4588	5.2415	(48,1/3)	30.0895	6.6800	(48,1/3)	31.4189	7.4234	(48,1/3)	30.7007
	"Hall"	5.9155	(48,1/3)	31.8640	5.0000	(48,1/3)	30.4669	6.3185	(48,1/3)	31.7148	6.8547	(48,1/3)	30.7007
	"Foreman"	9.3705	(48,1/3)	29.6126	9.6730	(48,1/3)	30.6207	10.4530	(48,1/3)	29.9952	13.0894	(48,1/3)	30.7007
	"Coastguard"	8.8500	(48,1/3)	28.2447	8.7360	(48,1/3)	28.9827	10.0510	(48,1/3)	28.6790	15.0000	(48,1/3)	30.7007
	Total	**41.2160**		**188.1517**	**40.0490**		**189.4016**	**44.7085**		**187.4228**	**53.9423**		**184.5402**
Case 4	"Akiyo"	5.0000	(48,1/3)	33.0309	5.0000	(48,1/3)	34.4020	5.0000	(48,1/3)	32.2495	5.0000	(48,1/3)	28.7813
	"Mother&Daughter"	5.8955	(48,1/3)	31.0128	5.8870	(48,1/3)	32.2639	6.1265	(48,1/3)	30.8076	6.5060	(48,1/3)	28.7813
	"Salesman"	6.2120	(48,1/3)	30.1727	6.1960	(48,1/3)	31.3233	6.5465	(48,1/3)	30.1503	7.2135	(48,1/3)	28.7813
	"Hall"	5.9260	(48,1/3)	30.5520	5.9170	(48,1/3)	31.7262	6.2070	(48,1/3)	30.4547	6.6985	(48,1/3)	28.7813
	"Foreman"	9.5655	(48,1/3)	28.4022	8.0570	(48,1/3)	27.4835	10.2450	(48,1/3)	28.5880	12.8005	(48,1/3)	28.7813
	"Coastguard"	9.0075	(48,1/3)	27.3516	7.5680	(48,1/3)	26.6678	9.5950	(48,1/3)	27.4337	13.6900	(48,1/3)	28.7813
	Total	**41.6065**		**180.5222**	**38.6250**		**183.8667**	**43.7200**		**179.6838**	**51.9085**		**172.6878**

at least one node receives a lower distortion and no node increases its distortion. Such a solution would result in a deviation from the "equilibrium". Thus, the lower distortion of one node would be a result of an increase of its transmission power. This would lead to an increase of the distortions of the other nodes. Therefore, an alternative solution where at least one node receives a lower distortion and no node increases its distortion cannot exist and the MMD leads to a Pareto-optimal solution.

For comparison reasons, each examined criterion, except for the PSO, it was also run using three competing optimization algorithms, for all cases of node distributions (see Section 6.1). Specifically, PSO's performance was compared with that of the deterministic algorithms AS [22,23], IP [24,25] and TRR [26,27]. Each of these methods was run for the same maximum number of function evaluations as PSO, i.e., 70,000 function evaluations. Furthermore, 30 independent experiments were also conducted for each one of the aforementioned deterministic methods, starting from a different, random starting point at each experiment, within the range [5.0, 15.0].

In the following, Tables 9–12 provide statistical information regarding the performance of all the aforementioned algorithms, over all independent trials. Specifically, each table presents the results for a particular bit rate and

bandwidth combination. The column "Case" refers to a specific node distribution. The column "Success" shows how many times each algorithm succeeds in finding the optimal solution to a precision of six decimal digits, out of 30 independent trials. Columns "Min", "Mean", "Max" and "Median" report the min, mean, max and median values of the function, respectively, over the 30 experiments. The standard deviation of the 30 values of the function is presented under the column "Std". We should note that for the NNBS and CNBS criteria the objective function is the one given by Eq. (12), assuming different bargaining powers for each of them. Similarly, the objective functions of the MAD and MMD criteria can be found in [16].

The last column of the tables presents the results of the Wilcoxon rank sum hypothesis tests [47,48], having set the significance level at 1%. More specifically, the obtained values of these tests can be either 1 or 0. A value equal to 1 indicates rejection of the null hypothesis at the 1% significance level, while a value equal to 0 indicates a failure to reject the null hypothesis at the 1% significance level. For each case of nodes' distribution, PSO was compared with the respective case of the AS, IP and TRR algorithms, and the results of the two-sided rank sum tests were reported under the "Ranksum" column, next to AS, IP and TRR algorithms, respectively. For example, for the case of

Table 9
Statistical results for PSO, AS, IP, TRR, $R_k=96$ kbps and $W_t=20$ MHz.

Criterion	Algorithm	Case	Success	Min	Mean	Max	Median	Std	Ranksum
NNBS	PSO	#1	30	−5.726552	−5.726552	−5.726552	−5.726552	0.00	–
		#2	30	−6.759974	−6.759974	−6.759974	−6.759974	0.00	–
		#3	29	−6.138522	−6.138506	−6.138032	−6.138522	0.00	–
		#4	24	−4.275103	−4.272522	−4.232132	−4.275103	0.01	–
	AS	#1	4	−5.726552	−0.121092	1.000000	1.000000	2.55	1
		#2	2	−6.759974	0.482668	1.000000	1.000000	1.97	1
		#3	4	−6.138522	0.048197	1.000000	1.000000	2.47	1
		#4	7	−4.275103	−0.582531	1.000000	1.000000	2.46	1
	IP	#1	6	−5.726552	−0.345310	1.000000	1.000000	2.74	1
		#2	1	−6.759974	0.482668	1.000000	1.000000	1.97	1
		#3	3	−6.138522	0.286148	1.000000	1.000000	2.18	1
		#4	9	−4.275103	−0.582531	1.000000	1.000000	2.46	1
	TRR	#1	0	−5.330930	−0.213350	1.000000	1.000000	2.28	1
		#2	0	−5.908247	0.565973	1.000000	1.000000	1.66	1
		#3	0	−4.873453	0.277376	1.000000	1.000000	1.88	1
		#4	0	−3.367513	−0.163746	1.000000	1.000000	1.82	1
CNBS	PSO	#1	30	−5.726552	−5.726552	−5.726552	−5.726552	0.00	–
		#2	30	−6.550393	−6.550393	−6.550393	−6.550393	0.00	–
		#3	30	−6.409900	−6.409900	−6.409900	−6.409900	0.00	–
		#4	30	−4.904941	−4.904941	−4.904941	−4.904941	0.00	–
	AS	#1	3	−5.726552	0.327345	1.000000	1.000000	2.05	1
		#2	2	−6.550393	0.496640	1.000000	1.000000	1.92	1
		#3	1	−6.409900	0.259011	1.000000	1.000000	2.26	1
		#4	7	−4.904941	−2.149301	1.000000	−4.904939	3.00	1
	IP	#1	4	−5.726552	0.103126	1.000000	1.000000	2.33	1
		#2	0	−6.550392	0.748320	1.000000	1.000000	1.38	1
		#3	1	−6.409900	0.259010	1.000000	1.000000	2.26	1
		#4	14	−4.904941	−1.755639	1.000000	1.000000	3.00	1
	TRR	#1	0	−4.964087	0.515564	1.000000	1.000000	1.51	1
		#2	0	1.000000	1.000000	1.000000	1.000000	0.00	1
		#3	0	−5.078231	0.442476	1.000000	1.000000	1.71	1
		#4	0	−4.420913	−0.777876	1.000000	1.000000	2.41	1
MAD	PSO	#1	29	27.877986	27.903443	28.641710	27.877986	0.14	–
		#2	30	22.105961	22.105961	22.105961	22.105961	0.00	–
		#3	30	25.335557	25.335557	25.335557	25.335557	0.00	–
		#4	28	38.152870	38.195643	38.921273	38.152872	0.17	–
	AS	#1	30	27.877986	27.877986	27.877986	27.877986	0.00	0
		#2	30	22.105961	22.105961	22.105961	22.105961	0.00	0
		#3	14	25.335557	27.840128	100.472675	25.335558	13.72	1
		#4	30	38.152872	38.152872	38.152872	38.152872	0.00	0
	IP	#1	27	27.877986	27.877986	27.877987	27.877986	0.00	0
		#2	30	22.105961	22.105961	22.105961	22.105961	0.00	0
		#3	14	25.335557	25.335558	25.335558	25.335558	0.00	1
		#4	30	38.152872	38.152872	38.152872	38.152872	0.00	0
	TRR	#1	0	35.459611	84.873294	590.658891	55.698445	105.48	1
		#2	0	29.444823	31,922,142.648722	957,609,654.693354	198.978964	174,834,459.25	1
		#3	0	29.759017	649.290198	13,790.047768	66.250344	2528.78	1
		#4	0	45.894814	97.197020	428.296977	60.885126	103.30	1
MMD	PSO	#1	26	32.630183	32.681779	33.238361	32.630183	0.16	–
		#2	30	27.063638	27.063638	27.063638	27.063638	0.00	–
		#3	20	28.211844	28.375334	29.236985	28.211844	0.33	–
		#4	29	45.627729	45.673158	46.990611	45.627729	0.25	–
	AS	#1	0	32.630184	32.727708	33.837196	32.630313	0.28	1
		#2	0	27.063640	27.214074	28.781947	27.064162	0.40	1
		#3	0	28.211845	28.277313	29.324319	28.214876	0.21	1
		#4	1	45.627729	45.627799	45.628617	45.627735	0.00	1
	IP	#1	0	32.893982	32.921179	33.593664	32.894431	0.13	1
		#2	0	27.286547	27.343641	27.381377	27.346057	0.01	1
		#3	0	28.475167	28.483026	28.513347	28.482314	0.01	1
		#4	0	45.992175	46.004366	46.080940	46.001779	0.01	1
	TRR	#1	0	63.809690	1473.410378	11,798.985887	735.239348	2557.98	1
		#2	0	50.968639	871.311987	3926.881004	561.712215	990.35	1
		#3	0	54.714794	5969.861550	162,460.812440	324.760820	29,562.79	1
		#4	0	63.999563	166.903248	491.288336	128.784483	96.83	1

Table 10
Statistical results for PSO, AS, IP, TRR, $R_k = 96$ kbps and $W_t = 15$ MHz.

Criterion	Algorithm	Case	Success	Min	Mean	Max	Median	Std	Ranksum
NNBS	PSO	#1	30	−5.931049	−5.931049	−5.931049	−5.931049	0.00	−
		#2	30	−6.884919	−6.884919	−6.884919	−6.884919	0.00	−
		#3	29	−6.357387	−6.357375	−6.357014	−6.357387	0.00	−
		#4	30	−4.644677	−4.644677	−4.644677	−4.644677	0.00	−
	AS	#1	10	−5.931049	−1.310350	1.000000	1.000000	3.32	1
		#2	11	−6.884919	−2.679628	1.000000	1.000000	4.00	1
		#3	2	−6.357387	−1.942954	1.000000	1.000000	3.67	1
		#4	2	−4.644677	−2.386805	1.000000	−4.644673	2.81	1
	IP	#1	14	−5.931049	−2.234490	1.000000	1.000000	3.52	1
		#2	13	−6.884919	−2.416798	1.000000	1.000000	3.97	1
		#3	18	−6.357387	−3.414432	1.000000	−6.357387	3.67	1
		#4	11	−4.644677	−1.069715	1.000000	1.000000	2.77	1
	TRR	#1	0	−5.622618	−2.655088	1.000000	−4.322057	2.89	1
		#2	0	−6.486487	−1.237290	1.000000	1.000000	3.24	1
		#3	0	−6.035897	−2.238168	1.000000	−3.305525	3.14	1
		#4	0	−4.130423	−1.386533	1.000000	−2.321361	2.17	1
CNBS	PSO	#1	30	−5.931049	−5.931049	−5.931049	−5.931049	0.00	−
		#2	19	−6.476440	−6.466387	−6.449022	−6.476440	0.01	−
		#3	16	−6.374505	−6.357740	−6.338579	−6.374505	0.02	−
		#4	30	−5.366147	−5.366147	−5.366147	−5.366147	0.00	−
	AS	#1	8	−5.931049	−1.541384	1.000000	1.000000	3.40	1
		#2	6	−6.476440	−0.744503	1.000000	1.000000	3.22	1
		#3	5	−6.374505	−0.229084	1.000000	1.000000	2.80	1
		#4	5	−5.366147	−1.970868	1.000000	1.000000	3.23	1
	IP	#1	16	−5.931049	−2.696559	1.000000	−5.931049	3.52	1
		#2	4	−6.476440	0.003141	1.000000	1.000000	2.58	1
		#3	9	−6.374505	−1.212352	1.000000	1.000000	3.44	1
		#4	14	−5.366147	−1.970869	1.000000	1.000000	3.23	1
	TRR	#1	0	−5.497558	−2.238326	1.000000	−3.878174	2.92	1
		#2	0	−5.926976	−0.693331	1.000000	1.000000	2.67	1
		#3	0	−5.030588	0.261632	1.000000	1.000000	1.92	1
		#4	0	−5.104637	−1.385651	1.000000	1.000000	2.80	1
MAD	PSO	#1	30	42.715334	42.715334	42.715334	42.715334	0.00	−
		#2	18	34.740266	34.741492	34.743331	34.740266	0.00	−
		#3	30	38.678888	38.678888	38.678888	38.678888	0.00	−
		#4	30	56.482854	56.482854	56.482854	56.482854	0.00	−
	AS	#1	8	42.715334	42.715335	42.715336	42.715335	0.00	1
		#2	27	34.740266	34.740266	34.740267	34.740266	0.00	1
		#3	17	38.678888	38.678888	38.678889	38.678888	0.00	1
		#4	8	56.482854	56.482855	56.482855	56.482855	0.00	1
	IP	#1	30	42.7715334	42.715334	42.715334	42.715334	0.00	0
		#2	11	34.740266	34.740267	34.740267	34.740267	0.00	0
		#3	30	38.678888	38.678888	38.678888	38.678888	0.00	0
		#4	30	56.482854	56.482854	56.482854	56.482854	0.00	0
	TRR	#1	0	48.597923	67.903578	124.637931	59.695320	21.60	1
		#2	0	41.072661	2,562,336.995613	76,818,946.290372	69.551001	14,024,836.44	1
		#3	0	41.140134	55.932004	84.065159	55.987149	9.81	1
		#4	0	59.823066	84.709830	142.269987	81.943355	21.17	1
MMD	PSO	#1	26	55.420774	55.516563	56.139190	55.420774	0.25	−
		#2	30	46.745971	46.745971	46.745971	46.745971	0.00	−
		#3	27	47.064096	47.260824	50.356854	47.064096	0.67	−
		#4	30	68.786486	68.786486	68.786486	68.786486	0.00	−
	AS	#1	0	55.420775	213,734.132136	6,410,416.730469	55.420789	1,170,366.50	1
		#2	2	46.745971	427404.773826	6410416.730469	46.746009	1626362.98	1
		#3	0	47.064097	47.414143	47.414143	47.064110	0.06	1
		#4	0	68.786488	68.954052	72.913638	68.786535	0.75	1
	IP	#1	0	55.788466	213,734.511989	6,410,416.730469	55.809086	1,170,366.43	1
		#2	0	47.116362	47.135636	47.155817	47.136172	0.01	1
		#3	0	47.373010	47.450356	47.459722	47.452354	0.01	1
		#4	0	69.178991	69.198662	69.198662	69.179764	0.00	1
	TRR	#1	0	93.225285	214,326.061791	6,410,416.730469	337.734698	1,170,255.19	1
		#2	0	78.373678	4090.934508	89,078.591611	343.627444	16,255.22	1
		#3	0	105.814688	433,327.625626	6,410,416.730469	279.925460	1,624,953.58	1
		#4	0	96.411897	181.725259	339.864507	149.604006	71.05	1

Table 11
Statistical results for PSO, AS, IP, TRR, $R_k = 144$ kbps and $W_t = 30$ MHz.

Criterion	Algorithm	Case	Success	Min	Mean	Max	Median	Std	Ranksum
NNBS	PSO	#1	28	− 5.600859	− 5.599407	− 5.579073	− 5.600859	0.01	–
		#2	22	− 6.723017	− 6.719601	− 6.710207	− 6.723017	0.01	–
		#3	30	− 6.062459	− 6.062459	− 6.062459	− 6.062459	0.00	–
		#4	25	− 4.144447	− 4.121988	− 3.845342	− 4.144447	0.07	–
	AS	#1	5	− 5.600859	− 0.760229	1.000000	1.000000	2.97	1
		#2	0	− 6.723015	0.742566	1.000000	1.000000	1.41	1
		#3	3	− 6.062459	− 0.177076	1.000000	1.000000	2.68	1
		#4	0	− 4.144446	− 0.200370	1.000000	1.000000	2.21	1
	IP	#1	10	− 5.600859	− 1.200286	1.000000	1.000000	3.16	1
		#2	1	− 6.723017	0.742566	1.000000	1.000000	1.41	1
		#3	5	− 6.062459	− 0.177076	1.000000	1.000000	2.68	1
		#4	7	− 4.144447	− 0.200371	1.000000	1.000000	2.21	1
	TRR	#1	0	− 5.020738	0.461282	1.000000	1.000000	1.65	1
		#2	0	− 4.769009	0.807700	1.000000	1.000000	1.05	1
		#3	0	− 5.326840	0.004166	1.000000	1.000000	2.27	1
		#4	0	− 3.502565	0.078349	1.000000	1.000000	1.71	1
CNBS	PSO	#1	28	− 5.600859	− 5.599407	− 5.579073	− 5.600859	0.01	–
		#2	30	− 6.572136	− 6.572136	− 6.572136	− 6.572136	0.00	–
		#3	29	− 6.255745	− 6.253124	− 6.177124	− 6.255745	0.01	–
		#4	25	− 4.746744	− 4.729444	− 4.584500	− 4.746744	0.05	–
	AS	#1	5	− 5.600859	− 0.760229	1.000000	1.000000	2.97	1
		#2	1	− 6.572136	0.747595	1.000000	1.000000	1.38	1
		#3	1	− 6.255745	0.274426	1.000000	1.000000	2.21	1
		#4	4	− 4.746744	− 0.340907	1.000000	1.000000	2.47	1
	IP	#1	10	− 5.600859	− 1.200286	1.000000	1.000000	3.16	1
		#2	1	− 6.572136	0.747595	1.000000	1.000000	1.38	1
		#3	3	− 6.255745	0.274425	1.000000	1.000000	2.21	1
		#4	7	− 4.746744	− 0.340907	1.000000	1.000000	2.47	1
	TRR	#1	0	− 5.020738	0.461282	1.000000	1.000000	1.65	1
		#2	0	− 3.896261	0.836791	1.000000	1.000000	0.89	1
		#3	0	− 4.803903	0.481003	1.000000	1.000000	1.59	1
		#4	0	− 4.448528	− 0.132917	1.000000	1.000000	2.10	1
MAD	PSO	#1	30	28.671136	28.671136	28.671136	28.671136	0.00	–
		#2	29	22.197505	22.203320	22.371955	22.197505	0.03	–
		#3	19	25.781431	25.795943	25.821008	25.781431	0.02	–
		#4	30	39.537574	39.537574	39.537574	39.537574	0.00	–
	AS	#1	29	28.671136	28.671136	28.671137	28.671136	0.00	0
		#2	30	22.197505	22.197505	22.197505	22.197505	0.00	0
		#3	23	25.781431	25.781431	25.781432	25.781431	0.00	0
		#4	2	39.537574	39.537575	39.537575	39.537575	0.00	1
	IP	#1	30	28.671136	28.671136	28.671136	28.671136	0.00	0
		#2	30	22.197505	22.197505	22.197505	22.197505	0.00	0
		#3	30	25.781431	25.781431	25.781431	25.781431	0.00	1
		#4	30	39.537574	39.537574	39.537574	39.537574	0.00	0
	TRR	#1	0	38.174917	80.084232	437.191990	54.975283	82.08	1
		#2	0	33.022878	115.806950	658.762104	61.160962	131.73	1
		#3	0	35.043037	136.701257	806.049917	74.006241	186.53	1
		#4	0	46.219864	65.138385	125.127617	59.559891	18.31	1
MMD	PSO	#1	14	31.056458	31.151369	31.355355	31.057992	0.13	–
		#2	26	24.095459	24.129881	24.612998	24.095459	0.12	–
		#3	15	27.066388	27.242809	28.630456	27.066426	0.40	–
		#4	29	44.347172	44.347172	44.347173	44.347172	0.00	–
	AS	#1	0	31.056462	31.078239	31.525284	31.056759	0.09	0
		#2	0	24.095463	24.135839	24.835710	24.095768	0.14	1
		#3	0	27.066398	27.224033	29.311025	27.072111	0.45	0
		#4	0	44.347187	44.419303	45.299474	44.352565	0.23	1
	IP	#1	0	31.241349	31.244034	31.245254	31.244358	0.00	1
		#2	0	24.279991	24.285232	24.287873	24.285217	0.00	1
		#3	0	27.228921	27.248421	27.259118	27.249201	0.00	1
		#4	0	44.524078	44.535475	44.598444	44.532140	0.01	1
	TRR	#1	0	94.109723	576.252212	3386.972994	288.327944	715.21	1
		#2	0	87.636164	605.994373	3050.645396	269.316773	740.79	1
		#3	0	45.631121	2812.207090	36,087.939245	627.444041	6679.12	1
		#4	0	61.519355	208.647801	439.313149	185.546088	93.59	1

Table 12
Statistical results for PSO, AS, IP, TRR, $R_k = 144$ kbps and $W_t = 22.5$ MHz.

Criterion	Algorithm	Case	Success	Min	Mean	Max	Median	Std	Ranksum
NNBS	PSO	#1	26	−6.728280	−6.706684	−6.317561	−6.728280	0.08	–
		#2	28	−7.817586	−7.817496	−7.814898	−7.817586	0.00	–
		#3	27	−7.198682	−7.167147	−6.771945	−7.198682	0.11	–
		#4	20	−5.259108	−5.158823	−4.178432	−5.259108	0.24	–
	AS	#1	3	−6.728280	−2.348921	1.000000	1.000000	3.90	1
		#2	7	−7.817586	−2.820954	1.000000	1.000000	4.44	1
		#3	5	−7.198682	−3.372630	1.000000	−7.198680	4.16	1
		#4	13	−5.259108	−2.129554	1.000000	−2.129553	3.18	0
	IP	#1	13	−6.728280	−2.348921	1.000000	1.000000	3.90	1
		#2	13	−7.817586	−2.820954	1.000000	1.000000	4.44	1
		#3	16	−7.198682	−3.372630	1.000000	−7.198682	4.16	1
		#4	15	−5.259108	−2.129554	1.000000	−2.129554	3.18	0
	TRR	#1	0	−5.920830	−1.691694	1.000000	1.000000	3.03	1
		#2	0	−7.072670	−2.070224	1.000000	1.000000	3.61	1
		#3	0	−6.461379	−2.447709	1.000000	−4.086208	3.33	1
		#4	0	−4.428599	−1.096080	1.000000	−0.021107	2.28	1
CNBS	PSO	#1	26	−6.728280	−6.706684	−6.317561	−6.728280	0.08	–
		#2	29	−7.494610	−7.494609	−7.494581	−7.494610	0.00	–
		#3	30	−7.247564	−7.247564	−7.247564	−7.247564	0.00	–
		#4	24	−5.968381	−5.879394	−5.345384	−5.968381	0.18	–
	AS	#1	3	−6.728280	−2.348921	1.000000	1.000000	3.90	1
		#2	7	−7.494610	−2.680997	1.000000	1.000000	4.28	1
		#3	14	−7.247564	−3.398701	1.000000	−7.247563	4.18	1
		#4	2	−5.968381	−2.484190	1.000000	−2.484189	3.54	1
	IP	#1	13	−6.728280	−2.348921	1.000000	1.000000	3.90	1
		#2	13	−7.494610	−2.680998	1.000000	1.000000	4.28	1
		#3	16	−7.247564	−3.398701	1.000000	−7.247564	4.18	1
		#4	15	−5.968381	−2.484190	1.000000	−2.484191	3.54	0
	TRR	#1	0	−5.920830	−1.691694	1.000000	1.000000	3.03	1
		#2	0	−6.353936	−1.683354	1.000000	1.000000	3.18	1
		#3	0	−6.700017	−2.361050	1.000000	−3.812727	3.26	1
		#4	0	−5.471234	−1.591104	1.000000	−0.546628	2.75	1
MAD	PSO	#1	30	56.480888	56.480888	56.480888	56.480888	0.00	–
		#2	30	44.424576	44.424576	44.424576	44.424576	0.00	–
		#3	30	50.564936	50.564936	50.564936	50.564936	0.00	–
		#4	30	78.125561	78.125561	78.125561	78.125561	0.00	–
	AS	#1	28	56.480888	56.480888	56.480889	56.480888	0.00	0
		#2	28	44.424576	44.424576	44.424577	44.424576	0.00	0
		#3	25	50.564936	50.564936	50.564937	50.564936	0.00	0
		#4	29	78.125561	78.125561	78.125562	78.125561	0.00	0
	IP	#1	30	56.480888	56.480888	56.480888	56.480888	0.00	0
		#2	30	44.424576	44.424576	44.424576	44.424576	0.00	0
		#3	30	50.564936	50.564936	50.564936	50.564936	0.00	0
		#4	30	78.125561	78.125561	78.125561	78.125561	0.00	0
	TRR	#1	0	70.058420	114.105190	305.226320	100.026179	49.94	1
		#2	0	55.440766	95.548555	265.978810	83.776112	42.75	1
		#3	0	62.454791	102.904933	297.469295	87.282984	50.16	1
		#4	0	94.335021	142.020580	313.279410	126.272882	52.33	1
MMD	PSO	#1	26	62.640217	62.674556	63.670340	62.640217	0.19	–
		#2	30	50.499656	50.499656	50.499656	50.499656	0.00	–
		#3	29	55.336279	55.446682	58.648373	55.336279	0.60	–
		#4	25	86.090121	86.138088	86.839018	86.090121	0.16	–
	AS	#1	0	62.640227	62.709359	64.231017	62.641429	0.29	1
		#2	0	50.499664	50.597425	52.681553	50.501584	0.40	1
		#3	0	55.336303	55.451090	56.332457	55.337953	0.28	1
		#4	0	86.090138	86.298447	88.117830	86.106936	0.49	1
	IP	#1	0	62.667073	62.689967	62.702033	62.691908	0.01	1
		#2	0	50.666813	50.843280	55.099470	50.695189	0.80	1
		#3	0	55.484306	56.219901	76.256342	55.529304	3.78	1
		#4	0	86.090126	86.249038	90.661932	86.090335	0.83	1
	TRR	#1	0	105.389738	661.950070	1853.695807	472.654046	473.79	1
		#2	0	104.554625	684.388187	1739.286364	533.403263	513.81	1
		#3	0	88.154391	650.196306	2273.759910	411.834949	534.75	1
		#4	0	131.077527	515.742949	1396.314830	392.958246	297.15	1

$R_k=96$ kbps and $W_t=20$ MHz, for the NNBS criterion, having "1" under the "Ranksum" column to Case 1 of AS, this means that the test rejects the null hypothesis of equal medians for the 30 values of the NNBS function using the PSO and the 30 values of the NNBS function using the AS, at 1% significance level.

Observing the successes of each optimization method over the 30 experiments for all considered bit rate and bandwidth combinations, we can see that PSO far exceeds the other methods, where in many cases its success rate is 100%. The great advantage of PSO compared to the other methods is more obvious in the MMD criterion. While PSO's success rate is in many cases 100%, the other methods fail nearly always to reach the optimal solution. However, there are a few cases where PSO's successes are less than 30. In these cases, if we examine the other statistic values of the tables, we will observe that the min value of the function differs from the max value (of the 30 values) in the third, second or first decimal digit. This claim is also confirmed by the small values of the standard deviation or by the fact that the min function value is equal with the median function value or have a slight difference in the fourth or third decimal digit. However, even in cases where PSO achieves a near-optimal solution, this solution is acceptable in practice, since it has only a slight impact on the utilities achieved by the nodes. Thus, all these statistical information reinforce our view about the efficiency of PSO in solving such optimization tasks.

Also, PSO, AS and IP behave better with the MAD criterion, noting better performance. As it was previously referred, PSO far exceeds the other competing methods, being able to nearly always reach the optimal solution. Among the benchmarks that we used for comparison with the PSO, the IP algorithm is the most efficient one, followed in performance by the AS, and finally, by the TRR, which fails always (in all examined cases) to reach the optimal solution.

The considerably low success rates of the deterministic algorithms can be probably attributed to the shape of the corresponding objective functions. Specifically, if they include steep hills as well as large flat areas, this can trap the deterministic approaches if they are initialized within these regions. This means that the selection of the starting point is very important for the performance of each method. For example, if the functions are flat in a large part, a starting point in this area does not lead any of the three above methods to find the optimal solution. This fact motivated us to use the PSO algorithm as the optimization solver in this paper.

Lastly, experimental results of the PSO's convergence speed are presented in Table 13. Specifically, this table shows the time that PSO requires to find the optimal solution with a precision of 6 decimal digits, in terms of the number of iterations that the swarm is updated. Thus, these statistics concern only the experiments where PSO reaches the optimal solution. In this table are included results for all node distributions of all considered bit rate and bandwidth combinations, and for all tested criteria. Due to the fact that PSO is a stochastic algorithm, we do not only cite the average performance, i.e., the mean number of iterations that the swarm is updated in order to reach the solution (Mean), but we also present the best case, i.e., the minimum number of iterations (Min) and the worst case, i.e., the maximum number of iterations (Max).

The criterion that presents the fastest PSO's convergence, requiring less iterations on average over all 30 experiments per case, is the MAD, which behaves better than all the other competing schemes. On the contrary, PSO confronts the biggest challenge in convergence, using the MMD criterion. With an exception for the case of $R_k=96$ kbps and $W_t=15$ MHz, in all other bit rate and bandwidth combinations, the MMD requires much more iterations on average compared to the other criteria. Especially when the bit rate is equal to 144 kbps, the

Table 13
PSO's convergence speed in terms of Best (Min), Average (Mean) and Worst (Max) swarm update iterations.

Bit rate – Bandwidth	Case	NNBS			CNBS			MAD			MMD		
		Min	Mean	Max	Min	Mean	Max	Min	Mean	Max	Min	Mean	Max
$R_k = 96$ kbps $W_t = 20$ MHz	#1	465	559.4	696	443	561.4	682	366	482.7	650	518	611.7	700
	#2	336	558.6	700	302	523.3	686	288	437.8	547	497	587.7	660
	#3	437	552.6	700	385	503.1	666	307	402.1	646	536	620.6	699
	#4	500	588.8	692	404	582.3	700	294	405.6	694	373	429.6	498
$R_k = 96$ kbps $W_t = 15$ MHz	#1	490	660.9	700	470	597.9	697	310	421.9	695	389	463.8	561
	#2	391	593.5	700	405	576.6	700	281	401.2	641	323	390.2	522
	#3	414	605.7	694	495	563.9	681	361	532.1	680	364	424.9	546
	#4	447	621.9	700	374	598.6	699	318	390.5	471	364	413.8	498
$R_k = 144$ kbps $W_t = 30$ MHz	#1	461	630.5	700	518	625.1	700	383	505.3	679	687	697.6	700
	#2	433	599.7	697	442	606.0	689	414	548.0	694	636	684.0	700
	#3	426	594.1	700	420	604.7	697	418	592.2	700	691	698.4	700
	#4	500	659.8	700	421	592.5	700	322	488.4	672	677	695.2	700
$R_k = 144$ kbps $W_t = 22.5$ MHz	#1	437	649.2	700	427	627.2	699	376	506.3	681	691	697.9	700
	#2	454	636.4	700	393	616.0	700	386	552.5	700	645	691.8	700
	#3	454	626.1	700	482	619.0	700	396	560.0	686	667	693.5	700
	#4	509	658.2	700	453	652.8	700	366	540.2	690	692	698.2	700

lowest average iteration number equals 684 out of 700 iterations.

7. Conclusions

In this work, we considered the problem of optimal resource allocation in wireless visual sensor networks. The source coding rate, channel coding rate, and power level were selected for each node of the network. Our setup assumed that the nodes negotiate with the help of a CCU, and the result of the negotiation is the NBS, which aims at a fair distribution of system resources among the nodes. The NBS utilizes a disagreement point, which corresponds to the minimum acceptable video quality for each node.

We proposed two optimization criteria based on the NBS, which differ in the way that the bargaining powers are determined for the nodes. The first approach treated each node as advantaged equally, while the second one assumed the same advantage for each class of nodes. The PSO algorithm was proved the best choice among other conventional optimization methods for solving the mixed-integer problems, resulting from the continuous values for the power levels and the discrete values for the source and channel coding rates, under the constraints of a fixed bit rate and a bounded power for each node.

The performance of our proposed criteria was compared with the performance of two other competing schemes, the MAD and MMD. The MAD criterion minimizes the average video distortion of the nodes without regard to fairness. The MMD criterion typically results in the same video distortion for all nodes, at the cost of a very high power consumption compared with the other schemes. This is a significant drawback of the MMD that could prohibit its use in practical applications. On the contrary, we confirmed that the NNBS and CNBS keep low computational complexity and can be used to any wireless VSN with a centralized topology that uses DS-CDMA. Additionally, a wise selection between NNBS and CNBS according to the needs of each application and the node distribution produces worthwhile results that are preferable to those of MAD and MMD.

Acknowledgments

References

[1] I. Menache, N. Shimkin, Noncooperative power control and transmission scheduling in wireless collision channels, in: Proceedings of the 2008 ACM SIGMETRICS International Conference on Measurement and Modeling of Computer Systems, SIGMETRICS '08, ACM, New York, NY, USA, 2008, pp. 349–358.

[2] T. Alpcan, T. Başar, R. Srikant, E. Altman, CDMA uplink power control as a noncooperative game, Wirel. Netw. 8 (2002) 659–670.

[3] Z. Han, K. Liu, Noncooperative power-control game and throughput game over wireless networks, IEEE Trans. Commun. 53 (2005) 1625–1629.

[4] Z. Han, Z. Ji, K.J.R. Liu, Power minimization for multi-cell ofdm networks using distributed non-cooperative game approach, in: Global Telecommunications Conference (GLOBECOM), IEEE, 2004, pp. 3742–3747.

[5] J. Suris, L. DaSilva, Z. Han, A. MacKenzie, R. Komali, Asymptotic optimality for distributed spectrum sharing using bargaining solutions, IEEE Trans. Wirel. Commun. 8 (2009) 5225–5237.

[6] M. Ahmed Khan, F. Sivrikaya, S. Albayrak, Network level cooperation for resource allocation in future wireless networks, in: Proceedings of the IFIP Wireless Days Conference '08, pp. 1–5.

[7] B. Yang, B. Shen, G. Feng, X. Guan, Fair resource allocation using bargaining over OFDMA relay networks, in: Proceedings of the 48th IEEE Conference on Decision and Control, 2009 Held Jointly with the 2009 28th Chinese Control Conference (CDC/CCC), pp. 585–590.

[8] J. Chen, A. Swindlehurst, Downlink resource allocation for multiuser MIMO-OFDMA systems: the Kalai–Smorodinsky bargaining approach, in: 3rd IEEE International Workshop on Computational Advances in Multi-Sensor Adaptive Processing (CAMSAP), pp. 380–383.

[9] H. Park, M. van der Schaar, Fairness strategies for wireless resource allocation among autonomous multimedia users, IEEE Trans. Circuits Syst. Video Technol. 20 (2010) 297–309.

[10] H. Park, M. van der Schaar, Bargaining strategies for networked multimedia resource management, IEEE Trans. Signal Process. 55 (2007) 3496–3511.

[11] N. Mastronarde, M. van der Schaar, A bargaining theoretic approach to quality-fair system resource allocation for multiple decoding tasks, IEEE Trans. Circuits Syst. Video Technol. 18 (2008) 453–466.

[12] E.S. Bentley, L.P. Kondi, J.D. Matyjas, M.J. Medley, B.W. Suter, Spread spectrum visual sensor network resource management using an end-to-end cross-layer design, IEEE Trans. Multimed. 13 (2011) 125–131.

[13] Q. Zhu, L. Pavel, End-to-end link power control in optical networks using Nash bargaining solution, in: Proceedings of the 2nd International Conference on Performance Evaluation Methodologies and Tools, ValueTools '07, ICST (Institute for Computer Sciences, Social-Informatics and Telecommunications Engineering), Brussels, Belgium, 2007, pp. 10:1–10:9.

[14] H. Yaiche, R.R. Mazumdarand, C. Rosenberg, A game theoretic framework for bandwidth allocation and pricing in broadband networks, IEEE/ACM Trans. Netw. 8 (2000) 667–678.

[15] H. Xu, B. Li, Efficient resource allocation with flexible channel cooperation in OFDMA cognitive radio networks, in: Proceedings of the 29th Conference on Information Communications, INFO-COM'10, IEEE Press, Piscataway, NJ, USA, 2010, pp. 561–569.

[16] K. Pandremmenou, L.P. Kondi, K.E. Parsopoulos, Optimal power allocation and joint source–channel coding for wireless DS-CDMA visual sensor networks, in: Proceedings of the SPIE Electronic Imaging Symposium (Visual Information Processing and Communication II), vol. 7882, San Francisco, CA, pp. 788206–788206-10.

[17] L.P. Kondi, E.S. Bentley, Game-theory-based cross-layer optimization for wireless DS-CDMA visual sensor networks, in: Proceedings of the 17th IEEE International Conference on Image Processing, Hong Kong, pp. 4485–4488.

[18] H.J.M. Peters, Axiomatic Bargaining Game Theory, Theory and Decision Library, Kluwer Academic Publishers, Dordrecht [u.a.], 1992.

[19] K. Pandremmenou, L.P. Kondi, K.E. Parsopoulos, Optimal power allocation and joint source–channel coding for wireless DS-CDMA visual sensor networks using the Nash bargaining solution, in: Proceedings of the 36th International Conference on Acoustics, Speech and Signal Processing, Prague, Czech Republic, pp. 2340–2343.

[20] H.Y. Benson, Using interior-point methods within an outer approximation framework for mixed integer nonlinear programming, in: J. Lee, S. Leyffer (Eds.), Mixed Integer Nonlinear Programming, The IMA Volumes in Mathematics and its Applications, vol. 154, Springer, New York, 2012, pp. 225–243.

[21] K.E. Parsopoulos, M.N. Vrahatis, Particle Swarm Optimization and Intelligence: Advances and Applications, Information Science Publishing (IGI Global), Hershey, PA, USA, 2010.

[22] P.E. Gill, W. Murray, M.H. Wright, Practical Optimization, Academic Press, London, UK, 1981.

[23] K. Schittkowski, An active set strategy for solving optimization problems with up to 200,000,000 nonlinear constraints, Appl. Numer. Math. 59 (2009) 2999–3007.

[24] R.H. Byrd, J.C. Gilbert, J. Nocedal, A trust region method based on interior point techniques for nonlinear programming, Math. Program. 89 (2000) 149–185.

[25] R.H. Byrd, M.E. Hribar, J. Nocedal, An interior point algorithm for large scale nonlinear programming, SIAM J. Optim. 9 (1997) 877–900.

[26] T.F. Coleman, Y. Li, An interior trust region approach for nonlinear minimization subject to bounds, Technical Report, Cornell University, Ithaca, NY, USA, 1993.

[27] T.F. Coleman, Y. Li, On the convergence of reflective newton methods for large-scale nonlinear minimization subject to bounds, Math. Program. 7 (1994) 189–224.

[28] K.S. Gilhousen, I.M. Jacobs, R. Padovani, A.J. Viterbi, L.A. Weaver, C. E. Wheatley, On the capacity of a cellular CDMA system, IEEE Trans. Veh. Technol. 40 (1991) 303–312.

[29] V.K. Garg, IS-95 CDMA and CDMA2000, Prentice Hall PTR, Upper Saddle River, NJ, USA, 2000.

[30] L.P. Kondi, F. Ishtiaq, A.K. Katsaggelos, Joint source–channel coding for motion-compensated DCT-based SNR scalable video, IEEE Trans. Image Process. 11 (2002) 1043–1052.

[31] Y.S. Chan, J. Modestino, A joint source coding-power control approach for video transmission over CDMA networks, IEEE J. Sel. Areas Commun. 21 (2003) 1516–1525.

[32] M. Dohler, S.A. Ghorashi, M. Ghozzi, M. Arndt, F. Said, A.H. Aghvami, Opportunistic scheduling using cognitive radio, Comptes Rendus Phys. 7 (2006) 805–815.

[33] S. Kaiser, OFDM-CDMA versus DS-CDMA: performance evaluation for fading channels, in: IEEE International Conference on Communications, ICC '95 Seattle, 'Gateway to Globalization', vol. 3, pp. 1722–1726.

[34] G.J. Sullivan, P. Topiwala, A. Luthra, The H.264/AVC advanced video coding standard: overview and introduction to the fidelity range extensions, in: SPIE Conference on Applications of Digital Image Processing XXVII, pp. 454–474.

[35] H. Wang, L.P. Kondi, A. Luthra, S. Ci, 4G Wireless Video Communications, Wiley Series on Wireless Communications and Mobile Computing, Wiley, Chichester, 2009.

[36] J. Hagenauer, Rate-compatible punctured convolutional codes (RCPC codes) and their applications, IEEE Trans. Commun. 36 (1988) 389–400.

[37] A. Viterbi, Convolutional codes and their performance in communication systems, IEEE Trans. Commun. Technol. 19 (1971) 751–772.

[38] W.H. Tranter, D.P. Taylor, R.E. Ziemer, N.F. Maxemchuk, J.W. Mark (Eds.), The Best of the Best: Fifty Years of Communications and Networking Research, Wiley/IEEE Press, Hoboken, NJ, USA, 2007.

[39] H. Schulzrinne, S.L. Casner, R. Frederick, V. Jacobson, RTP: A Transport Protocol for Real-Time Applications, IETF Request for Comments: RFC 3550, 2003.

[40] R. Zhang, S.L. Regunathan, K. Rose, Video coding with optimal inter/ intra-mode switching for packet loss resilience, IEEE J. Sel. Areas Commun. 18 (2000) 966–976.

[41] K. Binmore, Playing for Real: A Text on Game Theory, Oxford University Press, New York, NY, USA, 2007.

[42] J. Kennedy, R.C. Eberhart, Particle swarm optimization, in: Proceedings of the IEEE International Conference on Neural Networks, vol. IV, IEEE Service Center, Piscataway, NJ, 1995, pp. 1942–1948.

[43] R.C. Eberhart, J. Kennedy, A new optimizer using particle swarm theory, in: Proceedings of the Sixth Symposium on Micro Machine and Human Science, IEEE Service Center, Piscataway, NJ, 1995, pp. 39–43.

[44] M. Clerc, J. Kennedy, The particle swarm-explosion, stability, and convergence in a multidimensional complex space, IEEE Trans. Evol. Comput. 6 (2002) 58–73.

[45] I.C. Trelea, The particle swarm optimization algorithm: convergence analysis and parameter selection, Infor. Process. Lett. 85 (2003) 317–325.

[46] ⟨http://trace.eas.asu.edu/yuv/⟩, 2013, Online (accessed 19.10.13).

[47] J.D. Gibbons, S. Chakraborti, Nonparametric Statistical Inference (Statistics: A Series of Textbooks and Monographs), 4th edition, CRC, New York, NY, USA, 2003.

[48] M. Hollander, D.A. Wolfe, Nonparametric Statistical Methods, 2nd edition, Wiley-Interscience, Hoboken, NJ, USA, 1999.